Audio test:

Termická analýza

02 Termogravimetrická analýza –Thermogravimetric Analysis (TGA)

Přednášející: Doc. Jiří Sopoušek

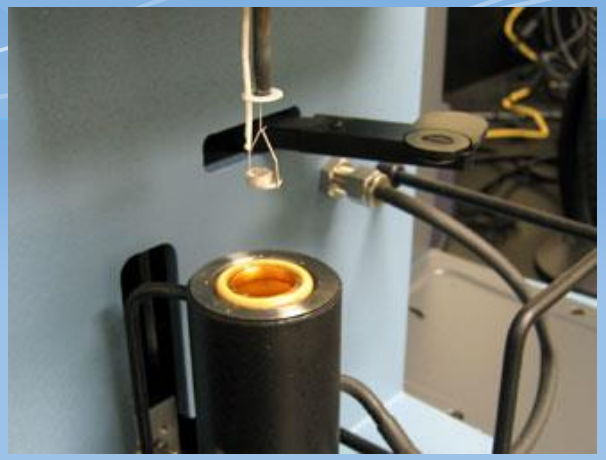

Princip

- Měření změn hmotnosti vzorku vystaveného změnám teploty (ohřev, chlazení, lineární, isotermická prodleva).

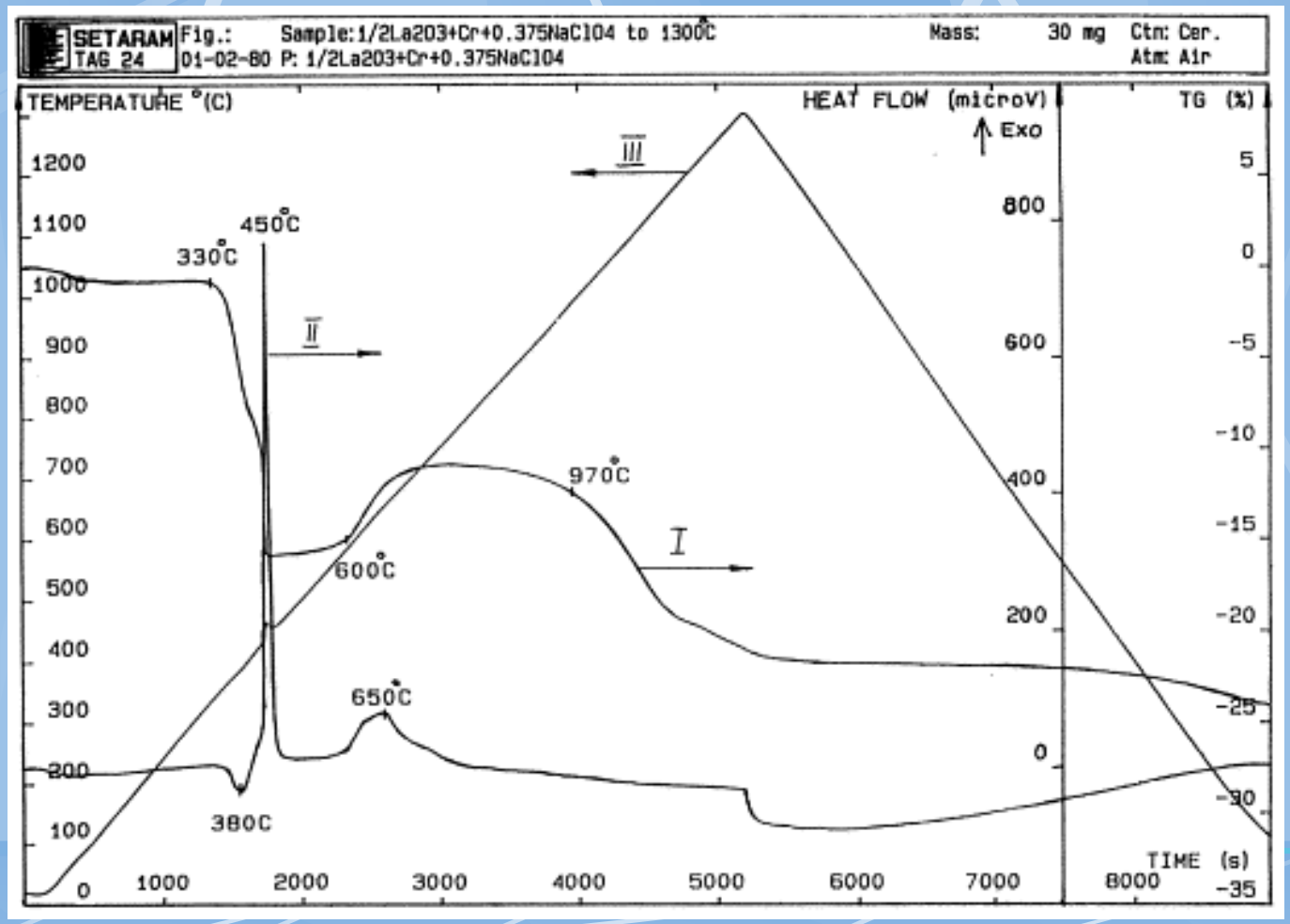

ICTAC definice TG

A technique in which the mass of the sample is monitored against time or temperature while the temperature of the sample, in a specified atmosphere, is programmed.

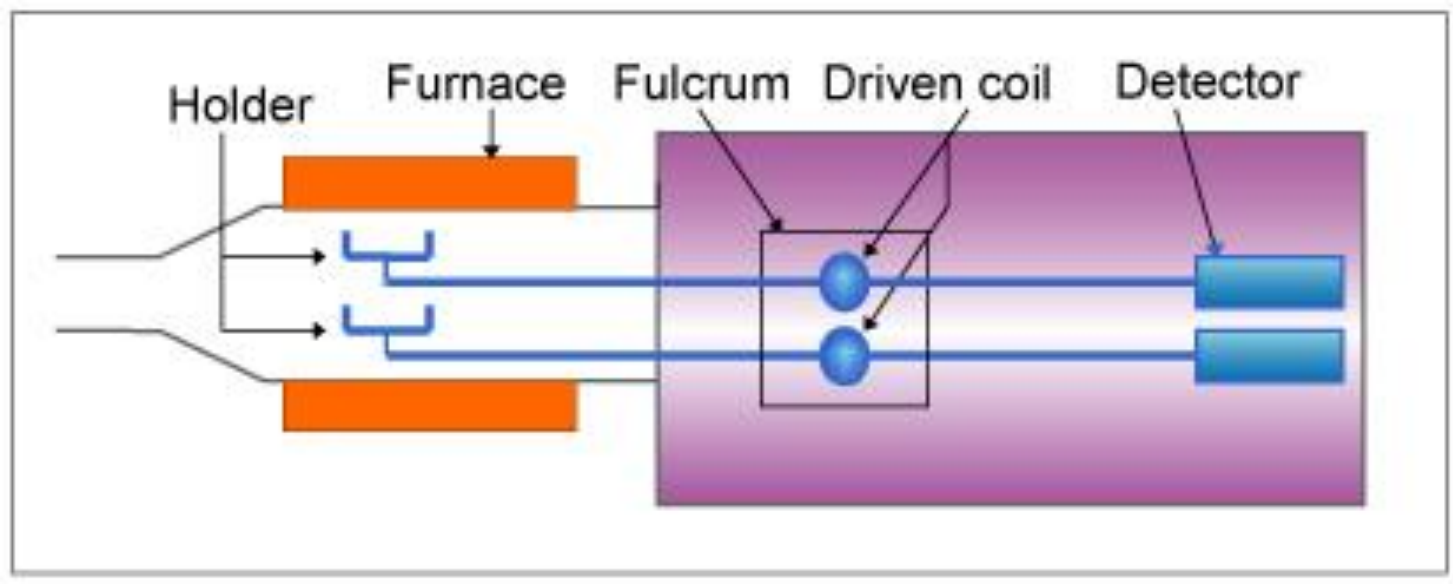

Použití

(všude, kde jde o změnu hmotnosti)

Například

- **Sledování těkavých látek (schnutí, desorpce, adsorpce, ztráta krystalové vody,…), měření čistoty látek (vlhkost)**
- **Oxidace na vzduchu nebo ve směsích s kyslíkem (kovy, oxidační rozklad organiky, ..)**
- **Termické rozklady v inertu, pyrolýza, karbonizace, …**
- **Heterogenní chemické reakce (produkt plynná složka)**
- **Reakce v redukční atmosféře**
- **Feromagnetické materiály (Magnetické vnější pole, Currie, Neel)**
- **Atd.**

Měřící uspořádání

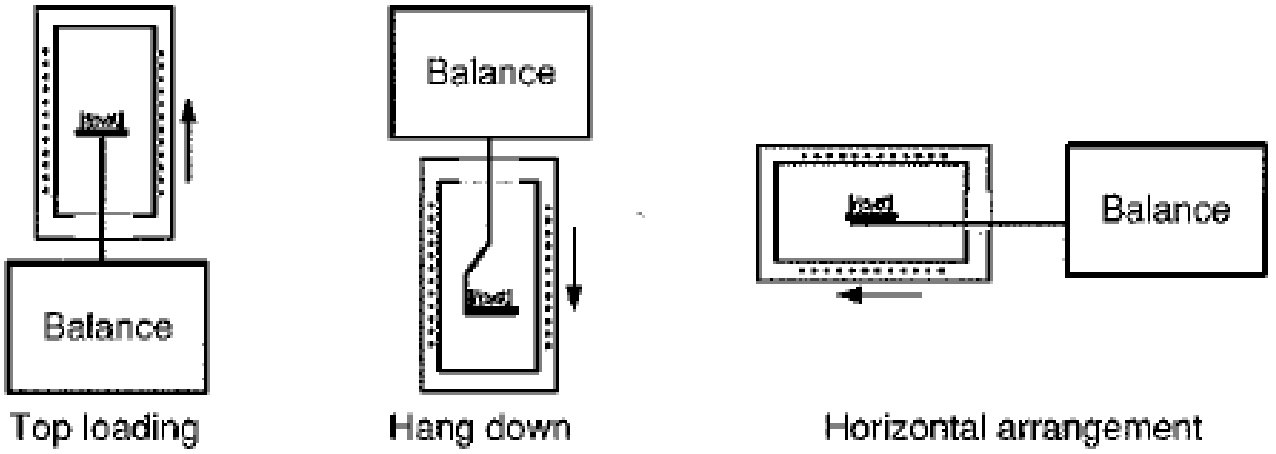

Figure 3.2 Thermobalance designs showing the top loading, hang down and horizontal arrangements.

Pozor na:

- **Zahřívání vah, ovlivnění nosným plynem**
- **Princip měření (klasický vs. elektronický)**
- **Koroze a poškozování závěsu**
- **Rozdíly v složení atmosférz v peci a ve vahách (proplachy, nelze vakuovat)**

Schéma měření TGA

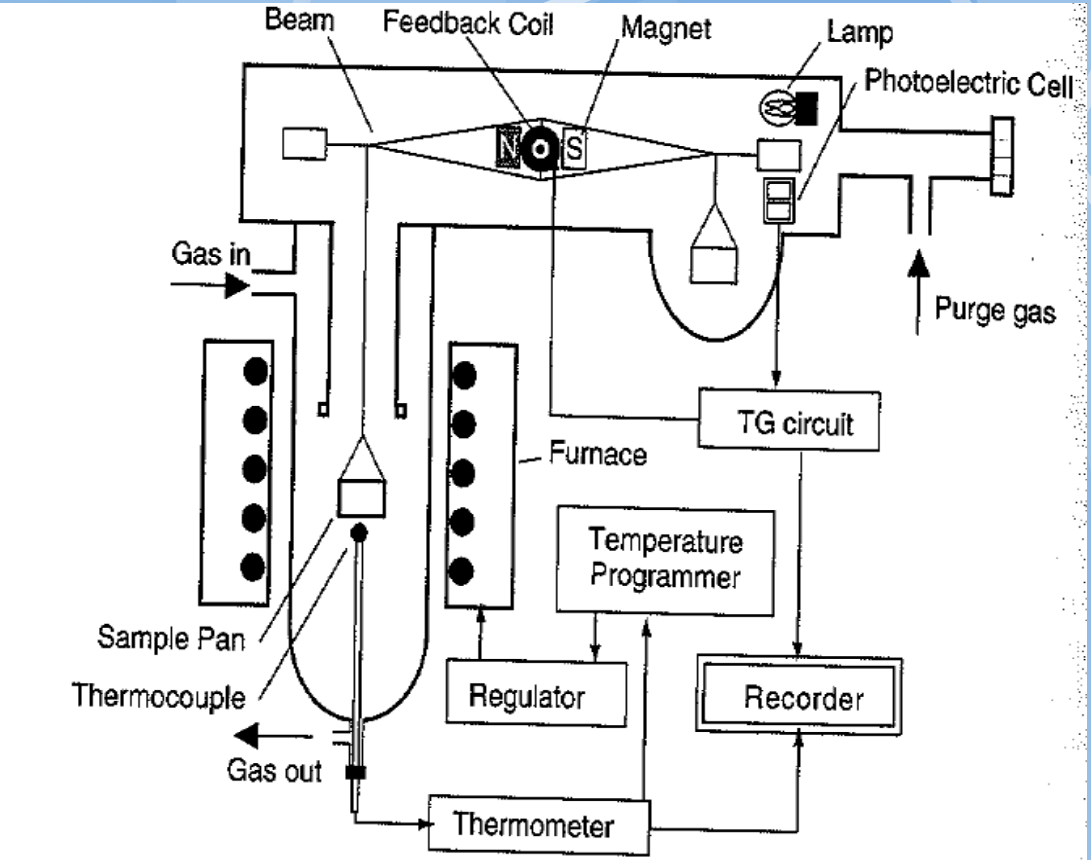

Figure 1 Schematic illustration of a TG apparatus of suspending type

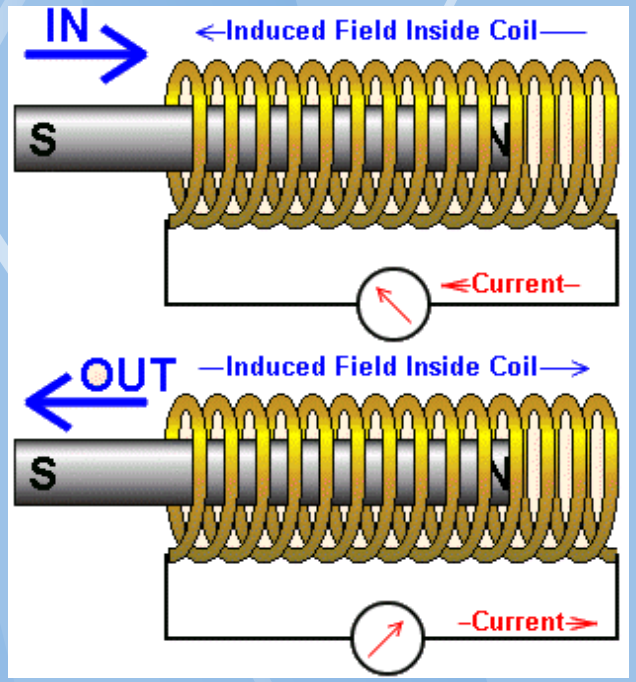

Nutno provádět kalibraci vah standardem hmotnosti.

Vertikální – horní váhy

Setaram

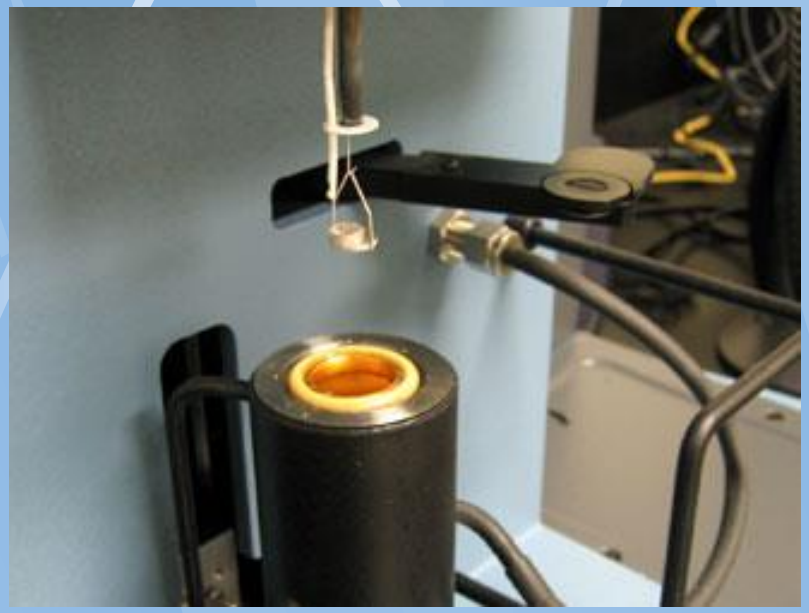

Horizontální TGA

TA instruments

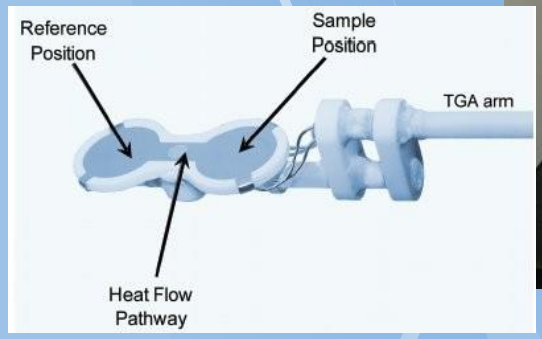

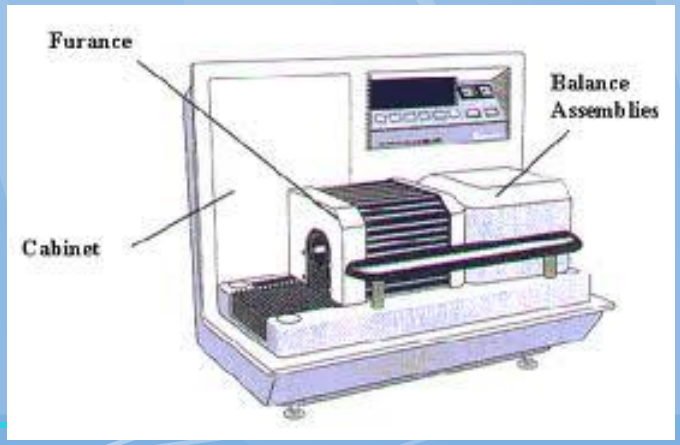

Verikální spodní váhy

Netzsch

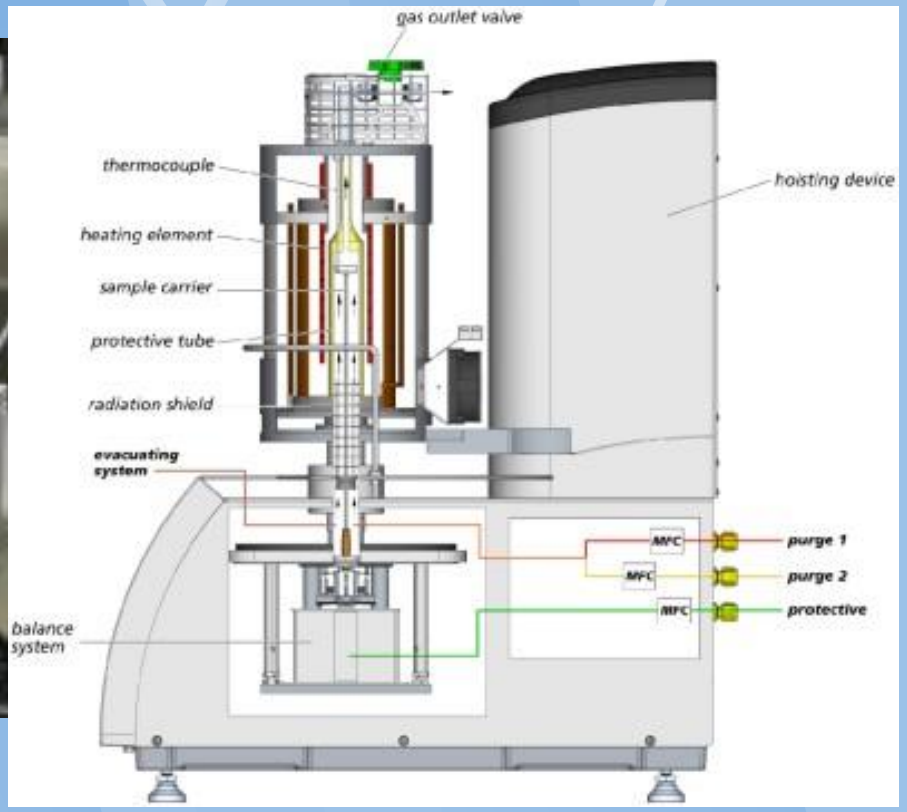

Rozklad šťavenanu vápenatého

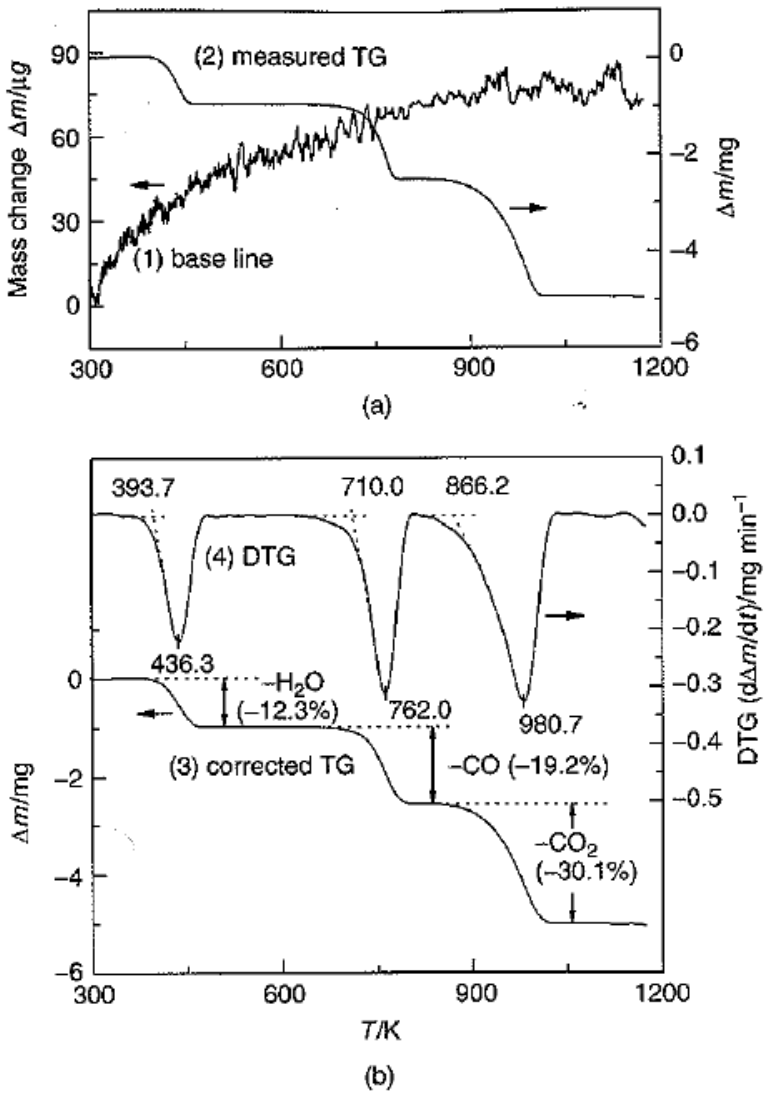

Figure 2 Analysis of TG curve as exemplified by the thermal decomposition of $CaC_2O_4 \cdot H_2O$

A: (100-226) °C, endo

$CaC_2O_4.2H_2O \rightarrow CaC_2O_4 + 2H_2O$

B1: (298-420) °C, v inertu, endo

$CaC_2O_4 \rightarrow CaCO_3 + CO$

B2: (289-420) °C, je-li O2, exo

$CaC_2O_4 + O_2 \rightarrow CaCO_3 + CO_2$

C: (660-840) °C, endo

$CaCO_3 + 1/2O_2 \rightarrow CaO + CO_2$

Pozn.: je to standardní látka , má velký povrch a čistí aparaturu

Způsob vyhodnocení

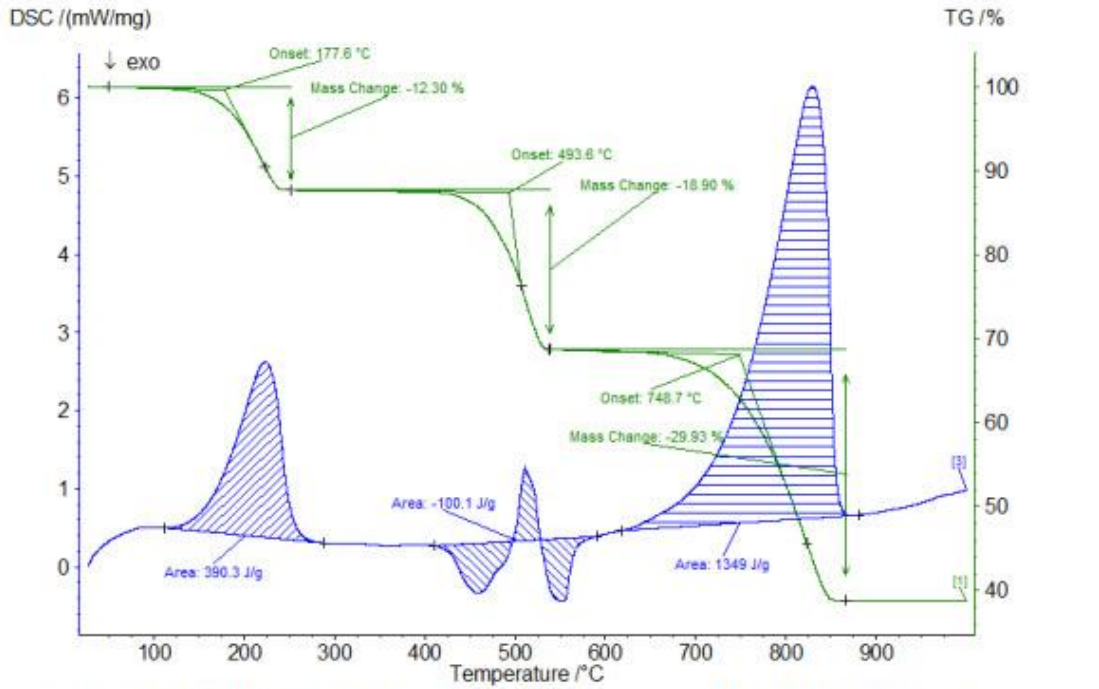

Figure 1. STA Data for the Decomposition of Calcium Oxalate Monohydrate.

Simultaneous Thermal Analysis (STA) – Ebatco

STA results for Calcium Oxalate Monohydrate, $CaC_2O_4 \cdot H_2O$; STA stands for simultaneous thermal analysis of DSC/DTA and TGA.

Table 1 Thermal Decomposition Reactions of Calcium Oxalate Monohydrate

Step	Reaction	Enthalpy (J/g)	Theoretical Mass Loss	Measured Mass Loss	% Error
1	$CaC_2O_4 \cdot H_2O \rightarrow CaC_2O_4 + H_2O$	390.3	12.33%	12.30%	-0.24%
2	$CaC_2O_4 \rightarrow CaCO_3 + CO$	-100.1	19.17%	18.90%	-1.41%
3	$CaCO_3 \rightarrow CaO + CO_2$	1349	30.12%	29.93%	-0.63%

DTGA

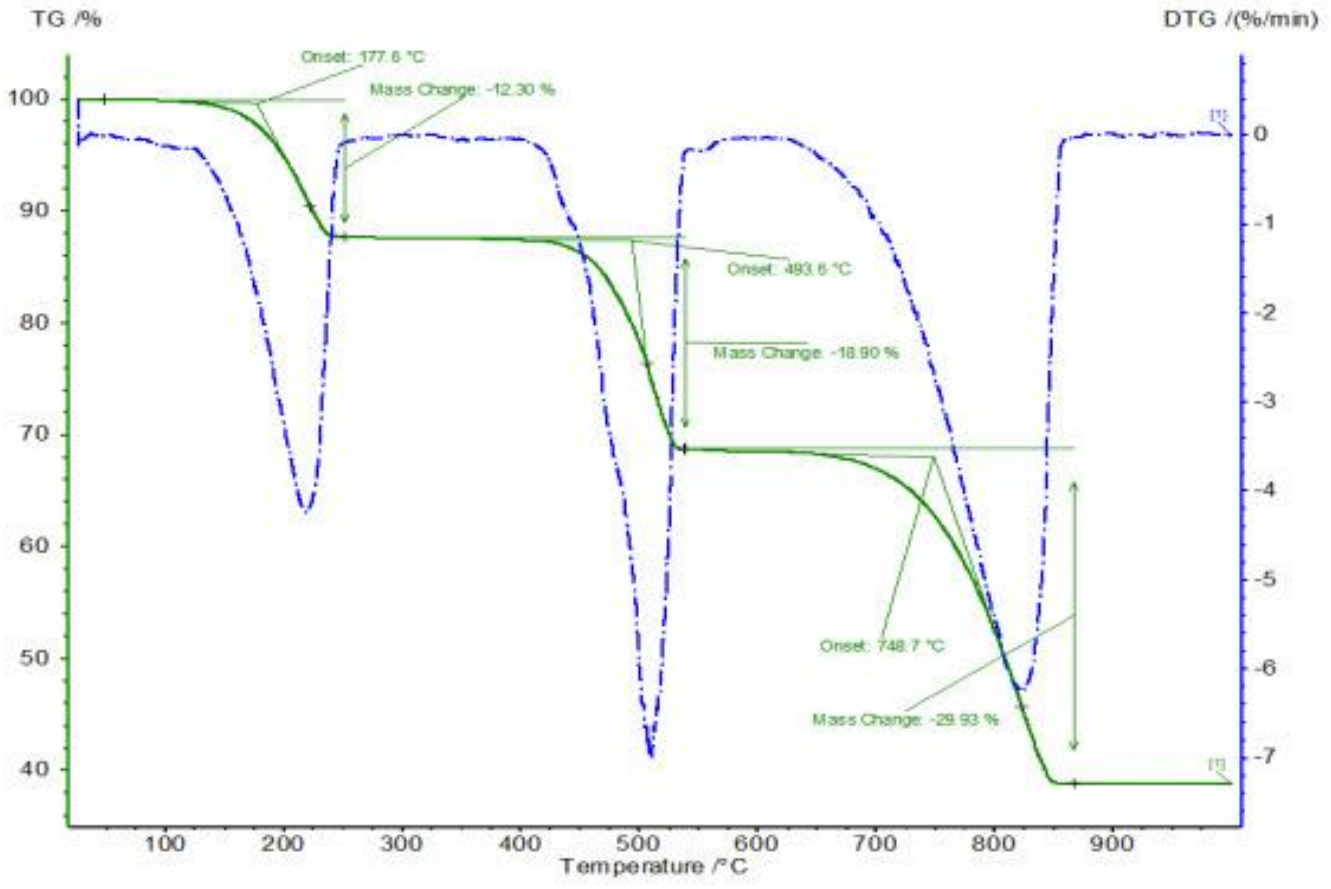

Figure 1. Thermal Decomposition of Calcium Oxalate Monohydrate.

Reakce CaC_2O_4 na $CaCO_3$ není triviální ale složená ze tří dějů.

Vliv nosného plynu na TGA křivku (oxidace a reaktivita !)

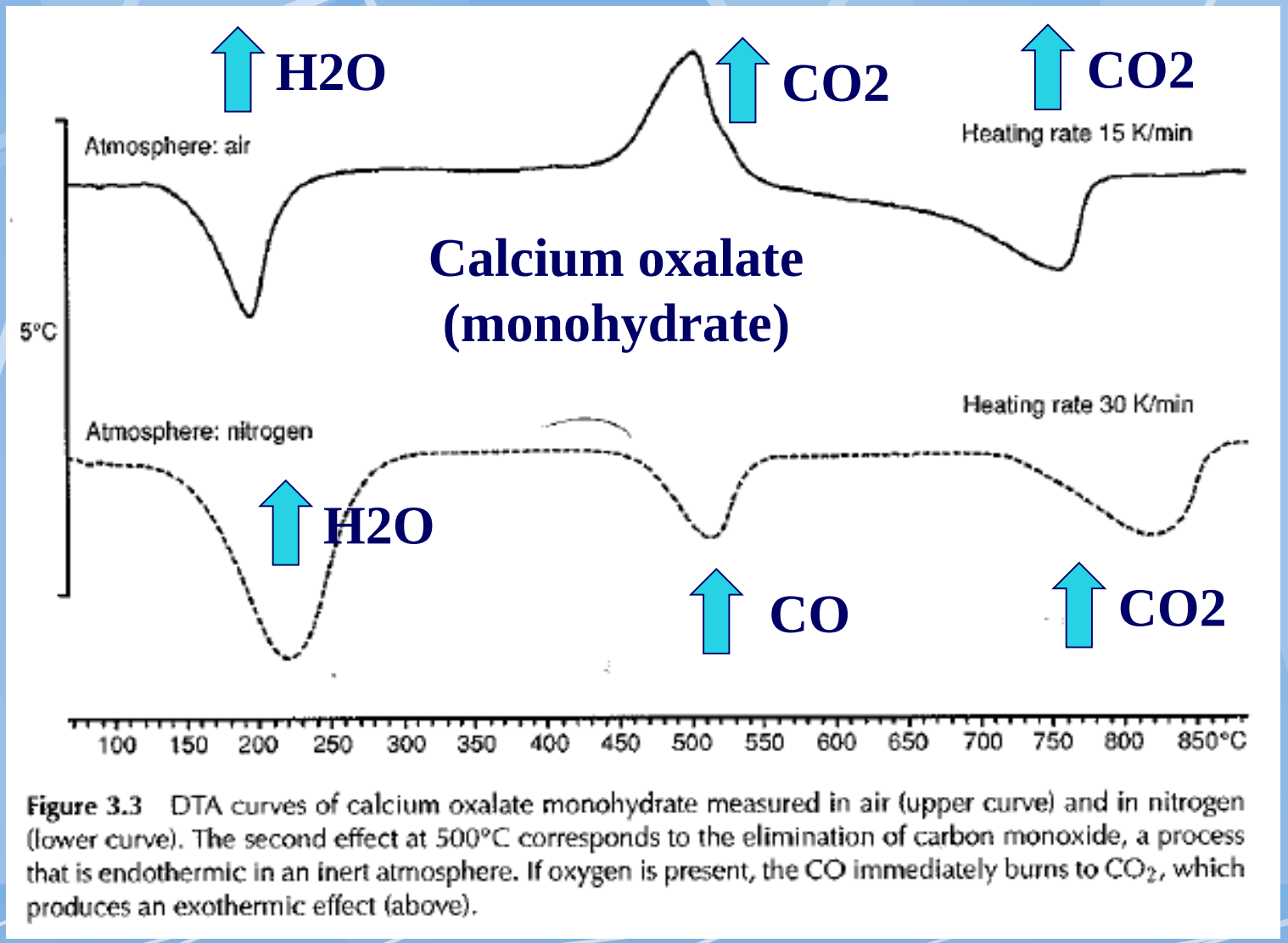

Figure 3.3 DTA curves of calcium oxalate monohydrate measured in air (upper curve) and in nitrogen (lower curve). The second effect at 500°C corresponds to the elimination of carbon monoxide, a process that is endothermic in an inert atmosphere. If oxygen is present, the CO immediately burns to CO_2, which produces an exothermic effect (above).

Korekce na vztlak

Korekci se vyhleme použitím wt%. Použijeme ji, pokud měníme plyn, nebo potřebujeme absolutní hmotnost.

Závisí na volbě nosného plynu

Table 3.1 Density of several gases at 25, 500 and 1000°C at a standard pressure of 101.3 kPa

Gas	Density (mg/mL) at 25°C	Density (mg/mL) at 500°C	Density (mg/mL) at 1000°C
Dry air	1.184	0.457	0.269
Nitrogen	1.146	0.441	0.268
Oxygen	1.308	0.504	0.306
Argon	1.634	0.630	0.383
Helium	0.164	0.063	0.038
Carbon dioxide	1.811	0.698	0.424

Vzorek při zahřívání „těžkne“

$$p = p_0 \frac{T_0}{T}$$

Ideal gass approx.

Nutná baseline s prázdným kelímkem pokud není korekce automatická díky SW

Příprava vzorku a podmínek experimentu

Representativní vzorek: jemný, přiměřená hmotnost, co nejméně poznamenat přípravou vč. kontaminace

Atmosféra: vhodná pro experiment, pozor na znečištění (O2, vlhkost, N2,.., redukční a oxidační potenciál,…), přetlak (0.05Atm), vhodná rychlost vznosu (funkce teploty), proplach vah (míšení s nosným plynem)

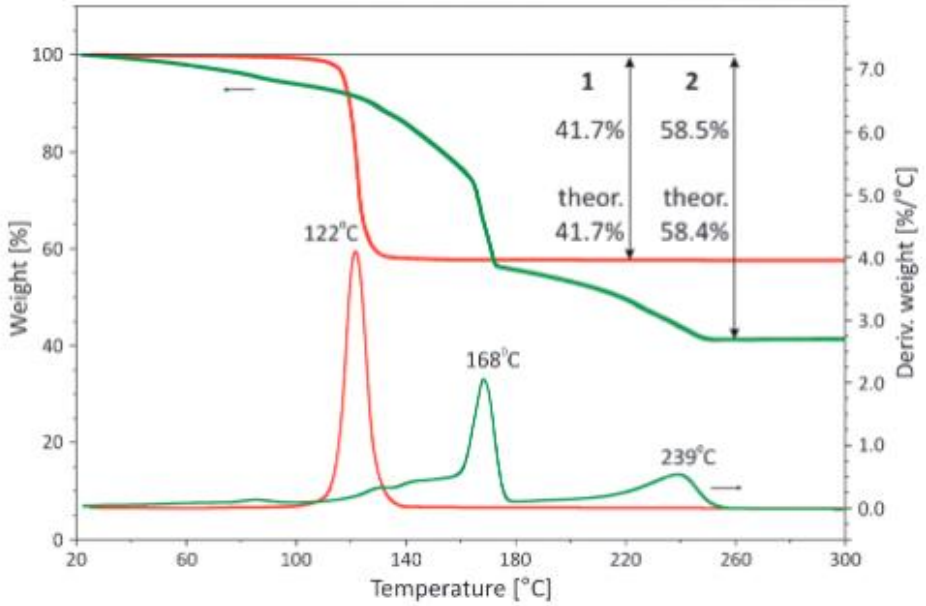

Fig. 2 Thermogravimetric analysis (TGA, DTG) traces showing the decomposition of compounds **1** and **2** in an inert (Ar) atmosphere.

Tert-Butylzinc hydroxide as an efficient predesigned precursor of ZnO nanoparticles (researchgate.net)

1…[tBuZn(m-OH)]n

2…tert-butoxide cluster (tBuZnOtBu)4

Obvyklé podmínky experimentu

- **Rychlost ohřevu** (10K/min, isoprodlevy,..), nastavení teplotního programu.
- **Nosný plyn** (inerty Ar, N2, synt. vzduch, He, …)
- **Alternativa: STA-sample controlled thermal analysis** (řízení rychlosti ohřevu změnou hmotnosti vzorku)
- **Měření baseline** (eliminuje řadu vlivů, ne např. emisivitu vzorku)

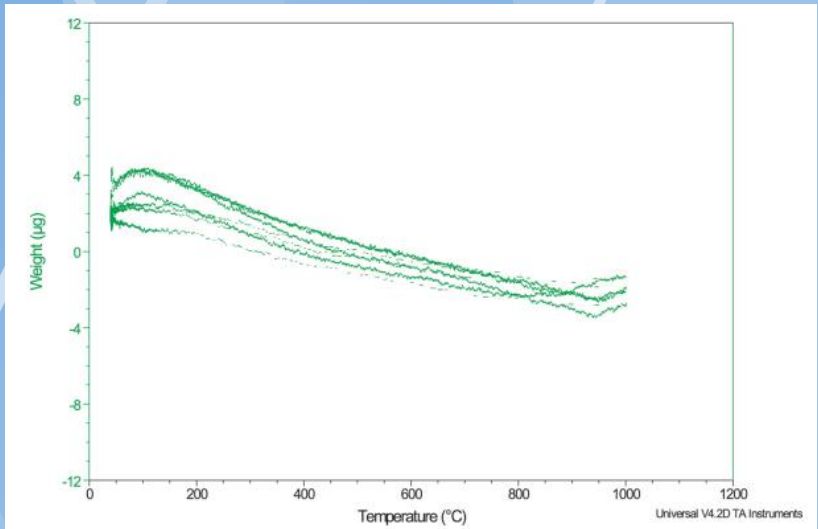

Figure 2 *Q5000 IR empty pan dynamic baselines.*

Layout 1 (tainstruments.com)

Volba rychlosti ohřevu

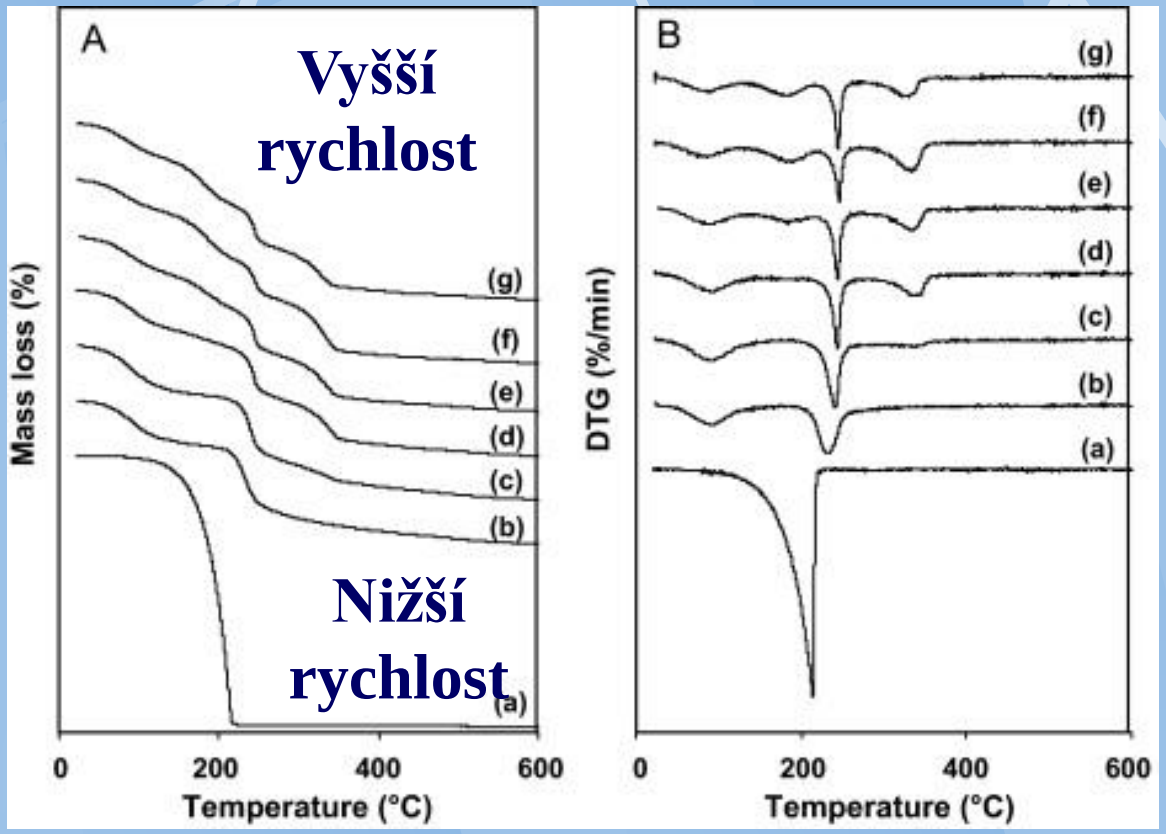

vyšší rychlosti posouvají reakce k vyšším teplotám

Isotermní prodlevy:

-na startu

-při měřených dějích

Vliv rychlosti ohřevu a STA-sample controlled thermal analysis

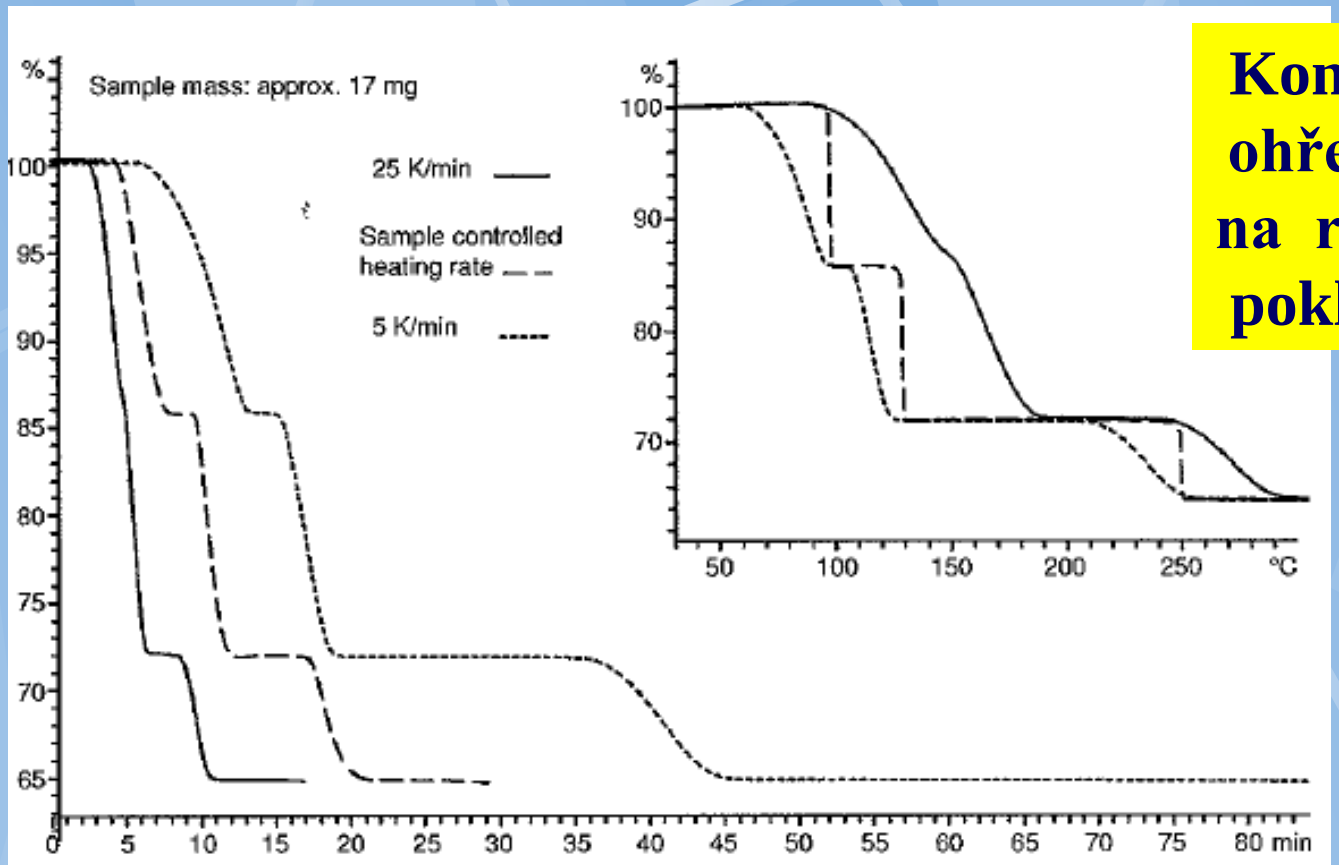

Figure 3.5 Influence of the heating rate on the resolution of partial reactions. In the inserted diagram on the right, the dotted and solid TGA curves of copper sulphate pentahydrate were measured conventionally at 5 and 25 K/min, whereas the dashed curve was recorded using the sample controlled heating rate. In this presentation of mass against temperature, the steps in the curve appear to be nearly vertical because, at low heating rates, the reaction takes place almost isothermally. In contrast, in the mass against time presentation (main diagram), the shapes of the three curves at first sight appear similar. On closer inspection, the better separation obtained using sample controlled heating rates – especially in the first two steps – becomes apparent.

Kontrola rychlosti ohřevu v závislosti na rychlosti změny poklesu hmotnosti

Změna hmotnosti a tepelné efekty TG-DTA pro jemné a hrubé krystaly

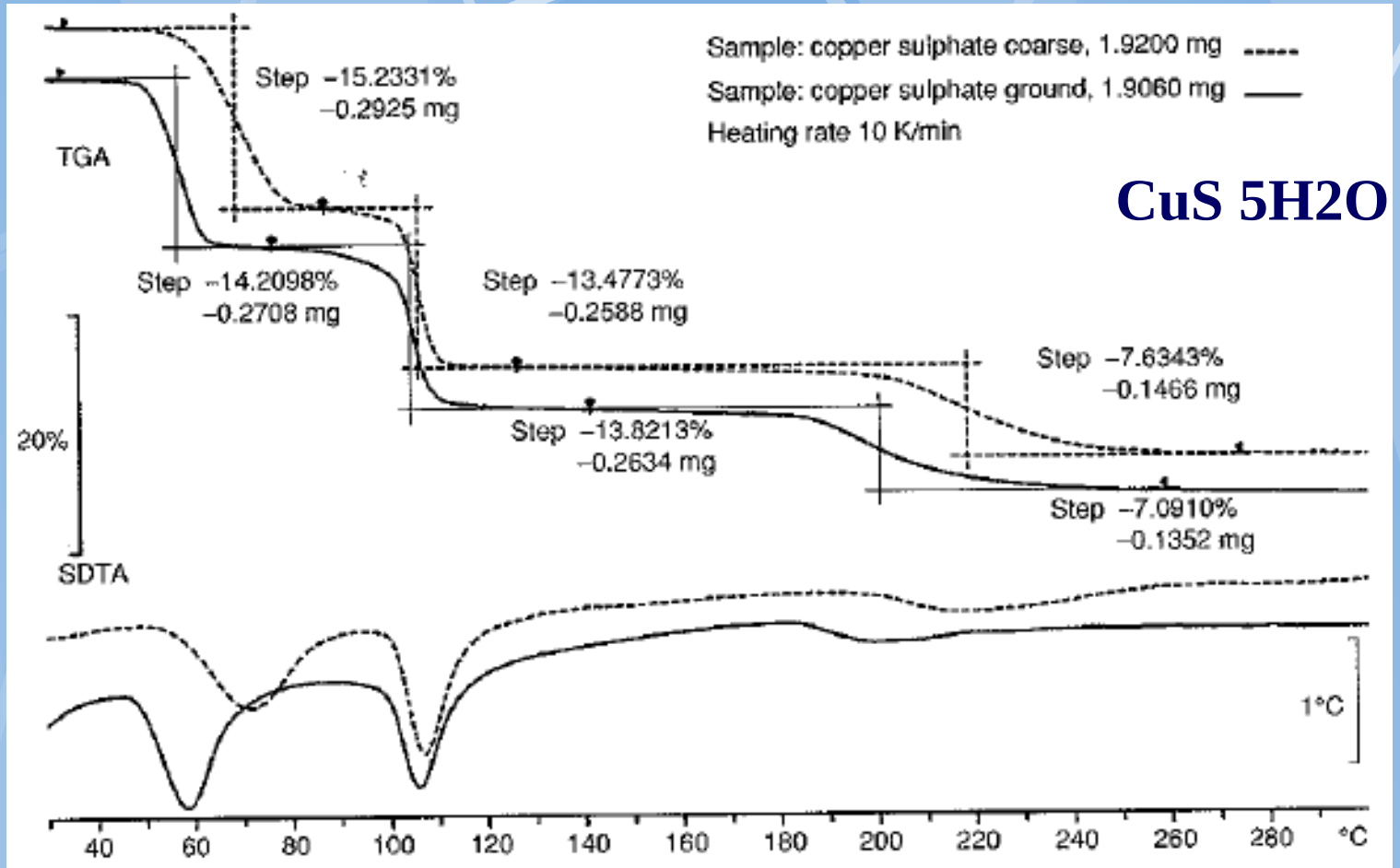

Figure 3.4 TGA and DTA curves showing the elimination of water of crystallisation from copper sulphate pentahydrate. The dotted curves were measured with rather coarse crystals, the solid curves with finely ground crystals. The first and third steps in the curve of the finely ground crystals are shifted more than 10 K to lower temperature. The heating rate was 10 K/min. Curves are offset for comparison.

Kelímky a atmosféra

Kelímky- nástřiky inertními oxidy (Al_2O_3, Y_2O_3)

Atmosféra (čisté plyny typicky 30ml/min inertu nebo S-air, 4%H_2+96%Ar, 20%O_2+80%N_2)

Pt

Safír

Alumina

Quartz

Čistota atmosfery - Zdroje znečištění kyslíkem

Table 3.2 Sources of residual oxygen and precautions

Sources of residual oxygen	Precautions
Oxygen content of the purge gas	Use an inert gas containing less than 10 ppm oxygen.
Leaks in the gas supply tubing and other fittings and connections	Oxygen can diffuse through plastic tubing! Either use very short sections of plastic tubing (less than 50 cm) or metal tubing with a minimum number of connections and joints. Carefully check all joints for leaks.
Outgassing of constructional components (oxygen adsorbed on parts of the measuring cell) and dead volume	Switch on the flow of protective gas to the microbalance several hours before measurement. Purge the vacuum connection as well. Only open the furnace briefly to insert the sample. Active replacement of air through slight evacuation to about 1 kPa. Then flood with the desired purge gas (if necessary twice).
Ingress of atmospheric oxygen due to leaks	A possible cause of leakage is the furnace seal which could be damaged or dirty.
Ingress of atmospheric oxygen due to back diffusion at the purge gas outlet	Attach a long narrow tube to the outlet (this functions as a diffusion baffle).

Vliv změn tlaku (na elastomer)

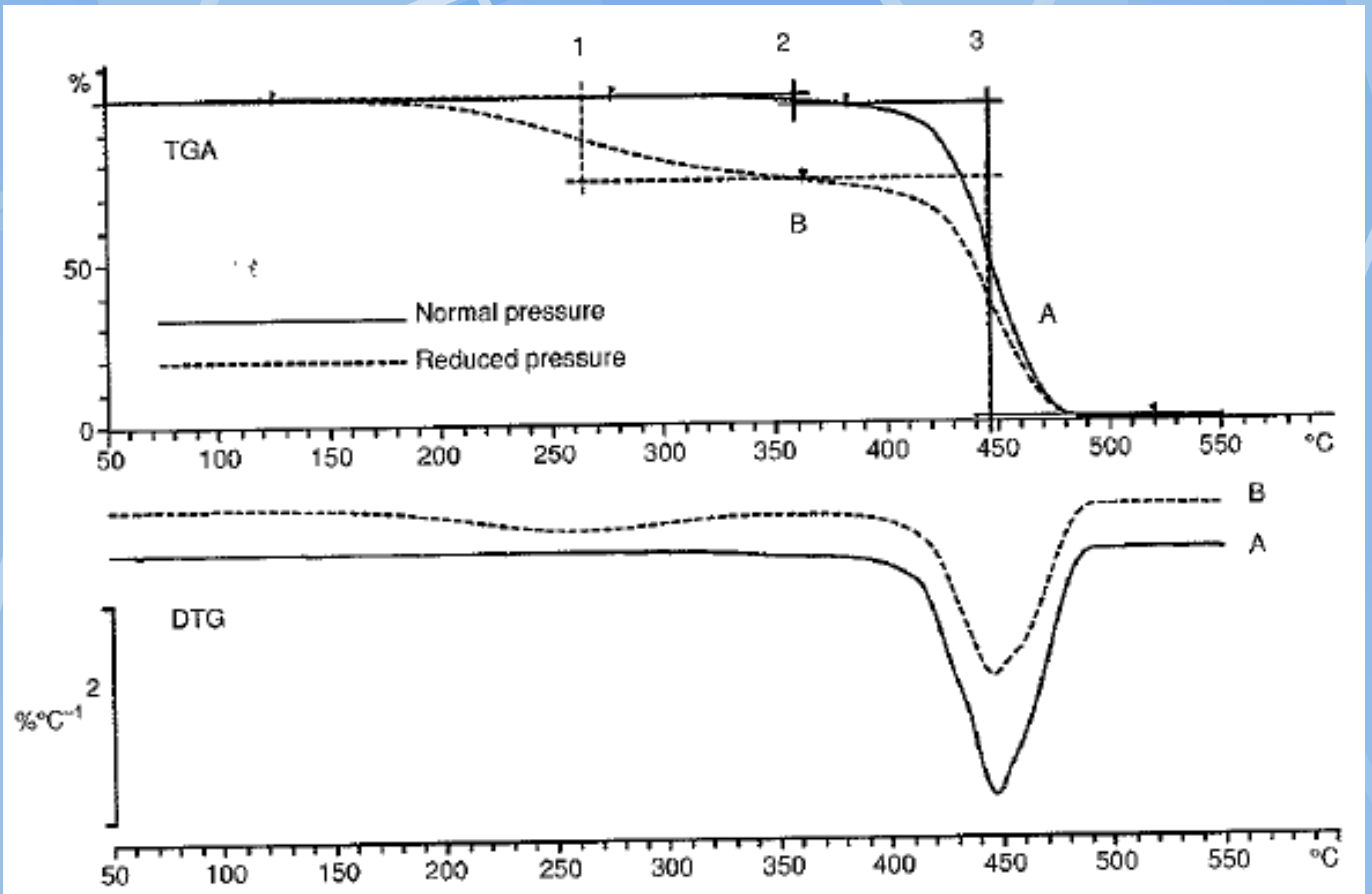

Figure 3.6 Effect of pressure on the decomposition of an elastomer: sample A is measured at normal (atmospheric) pressure, and B under reduced pressure, 1.5 kPa (15 mbar). Under reduced pressure, the vaporisation of the volatile components (additives, 1) is clearly separated from the decomposition of the elastomer (2,3). At normal pressure, the step height evaluated (on an expanded scale) from the stable region of the baseline at 270°C to next DTG maximum at 380°C does not correspond to the true additive content.

Další vlivy

- **vliv vlhkosti (dobře prožíhané kelímky!!!!!!!!!!!!,)**
- **Zbytky vlhkosti v nosném plynu způsobyjí adsorpční parazitní efekty.**
- **Autosampler (Al kelímky nejlépe, kapsulovat s dírkou)**

Interpretace záznamů TGA

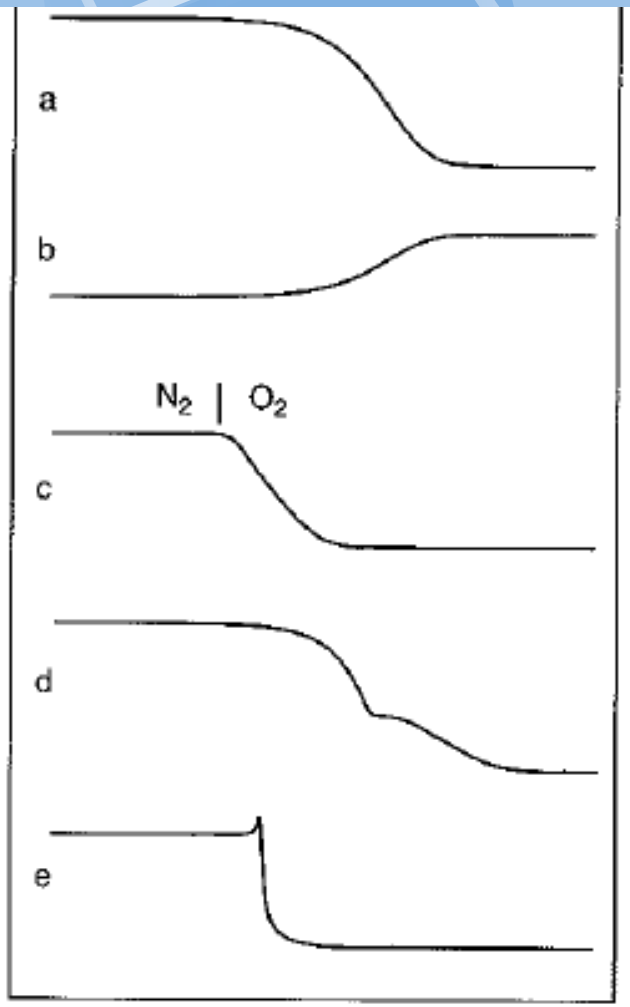

Figure 3.7 TGA curves of different chemical reactions. (a) Thermal decomposition with the formation of volatile reaction products. (b) Corrosion, oxidation of metals (formation of non-volatile oxides). (c) Combustion of carbon black on switching from N_2 to O_2. (d) Multi-step decomposition. (e) Explosive decomposition with recoil effect.

Termický rozklad

Oxidace

„Zhoření“

Výcestupňový rozklad

„Výbuch“

Přítomnost chemické reakce

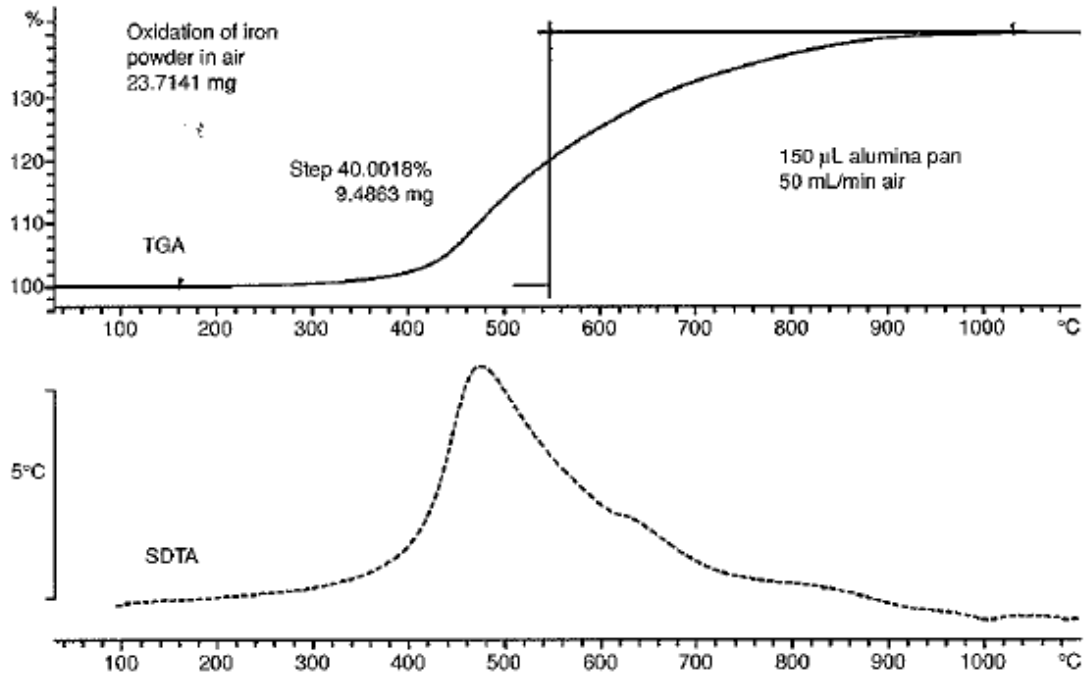

Figure 3.8 Example of a chemical reaction with an increase in mass. The iron powder takes up 40% oxygen in air and forms Fe_3O_4 and Fe_2O_3. The SDTA curve below confirms that the reaction is strongly exothermic; heating rate 20 K/min, Al_2O_3 crucible 150 µL. This reaction has an exceptionally wide temperature range of 600 K for 1–99% conversion.

Rozklad aspartanu

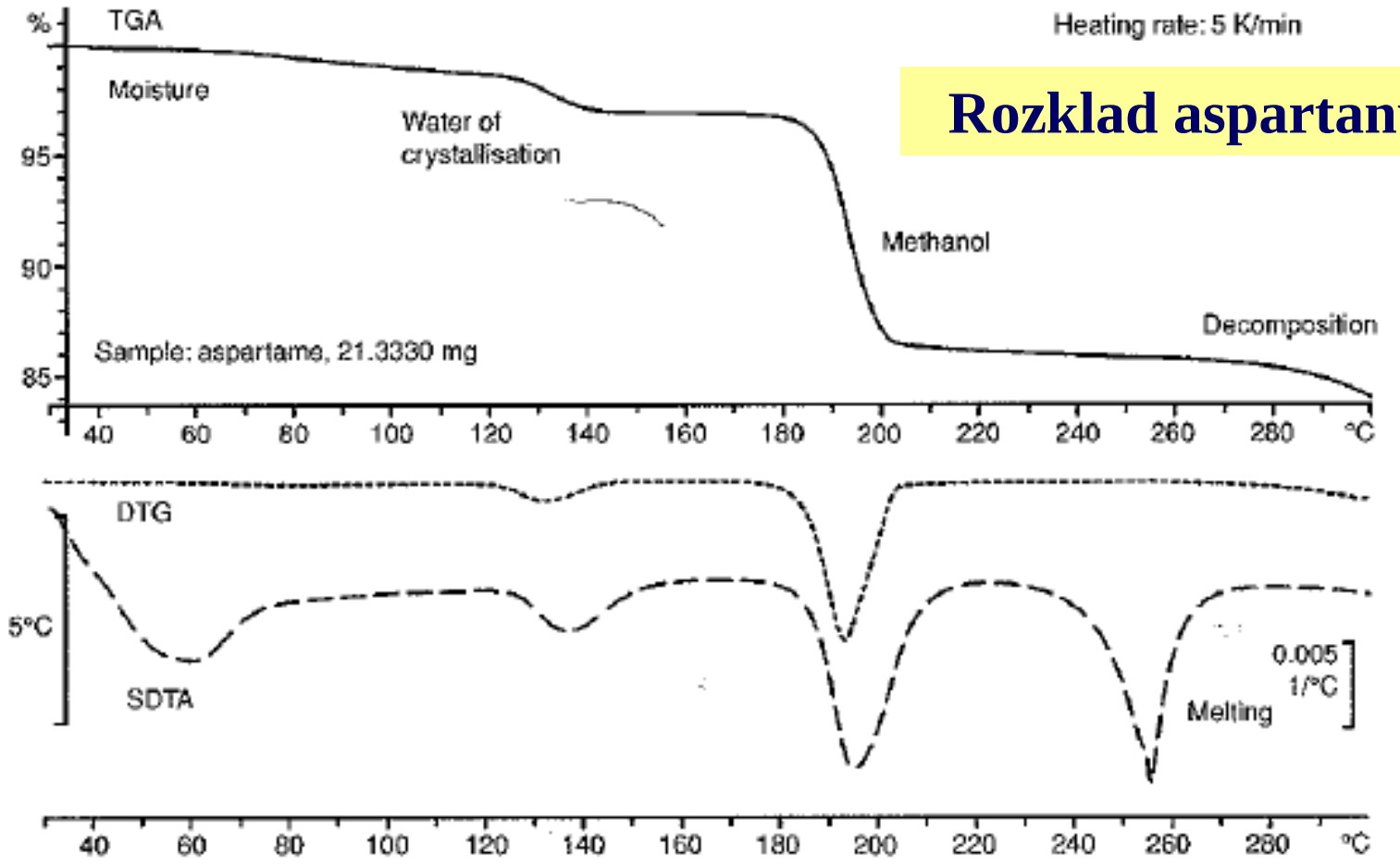

Figure 3.9 The decomposition of the artificial sweetener aspartame appears to be relatively complex. First, the water of crystallisation is lost at about 130°C. This is followed by the elimination of methanol at 180°C and the formation of a piperazine ring. This reaction takes place in an extremely narrow temperature range of just 20 K for 1–99% conversion. The SDTA curve shows that the piperazine derivative melts at 250°C.

Taní na TG křivce

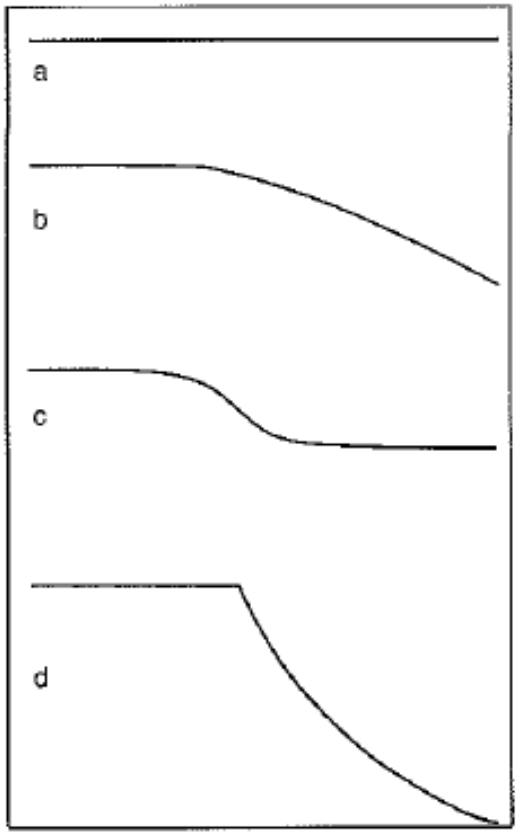

Figure 3.10 Thermogravimetric effects on melting. (a) Sample with low vapour pressure (no TGA effect). (b) Volatile melt (the liquid sample evaporates). (c) Moisture escapes on melting. (d) Sample melts and decomposes.

OK

Malý odpar (Zn, Se, ..)

Ztráta něčeho při tání (vlhkost)

Taní spojené s rozkladem

Další efekty

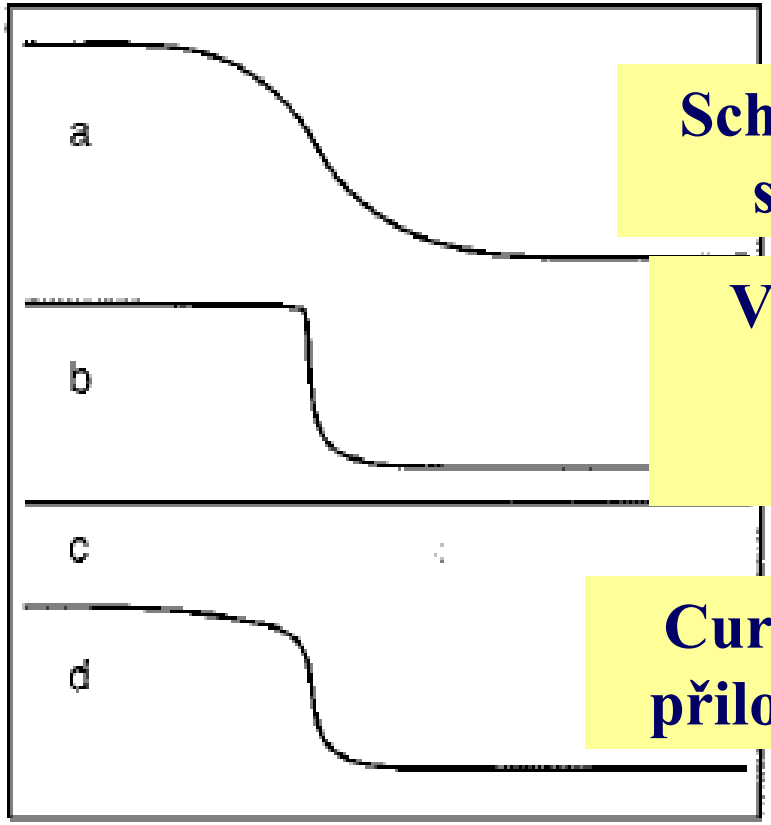

Schnutí, desorpce, sublimace,…

Var a malá dirka (další skok = odfouknutí)

Currie a Neel při přiložení magnetu

Figure 3.12 Other thermogravimetric effects. (a) Drying, desorption, sublimation. (b) Boiling in a crucible with a small hole in the lid. (c) Ferromagnetic Curie transition without a magnet: no TGA effect. (d) The same sample with a permanent magnet below the furnace.

Vliv rychlosti t na magnetické efekty

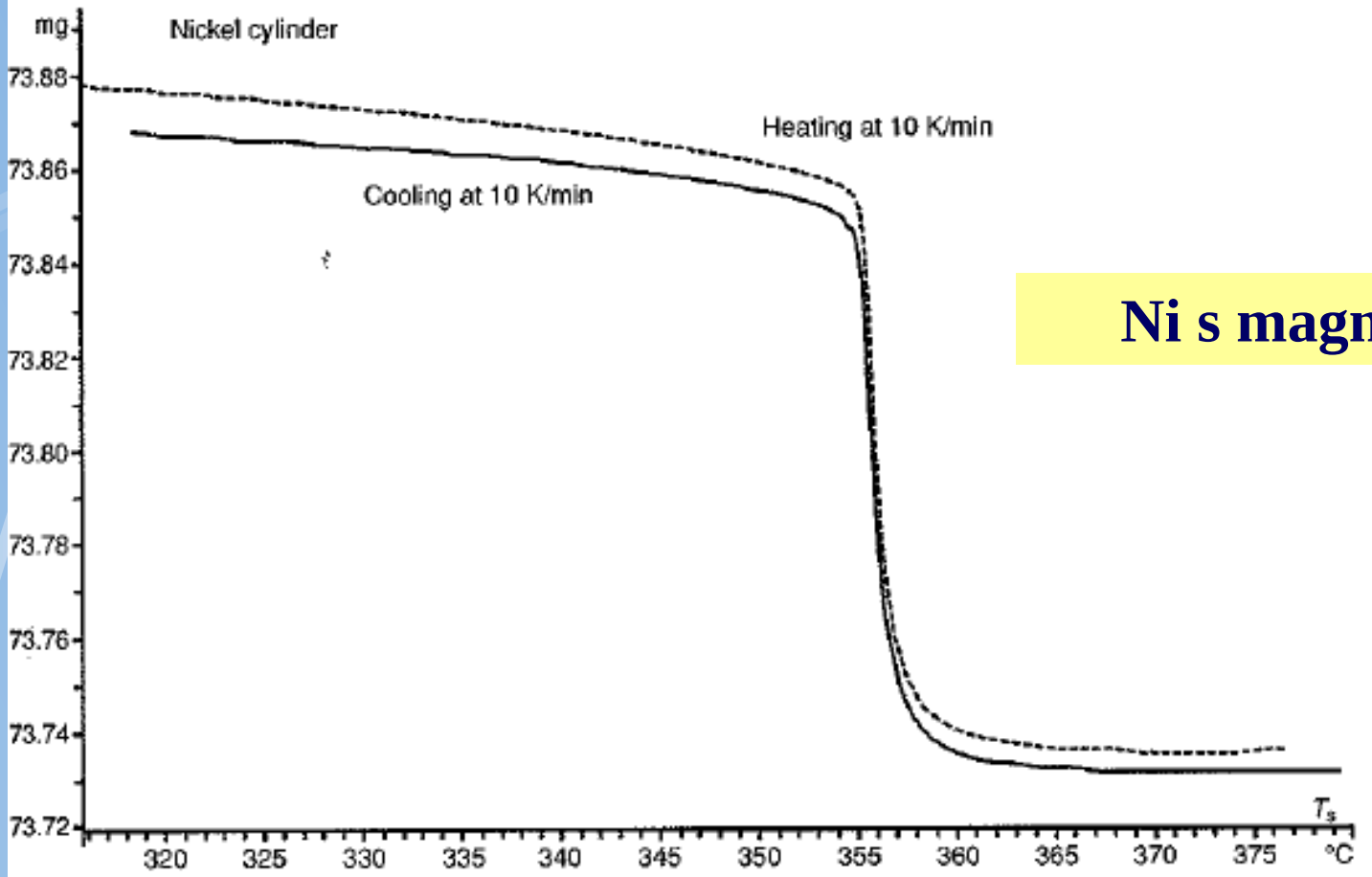

Figure 3.13 A permanent magnet placed below the furnace of the thermobalance attracts a ferromagnetic material and causes an apparent increase in mass. When the Curie temperature of the sample is exceeded, the force is no longer exerted and there is a sudden loss in apparent mass. This effect is reversible and occurs again on cooling. The abscissa shows the sample temperature, T_s.

Ni s magnetem

Vyhodnocení křivek TG

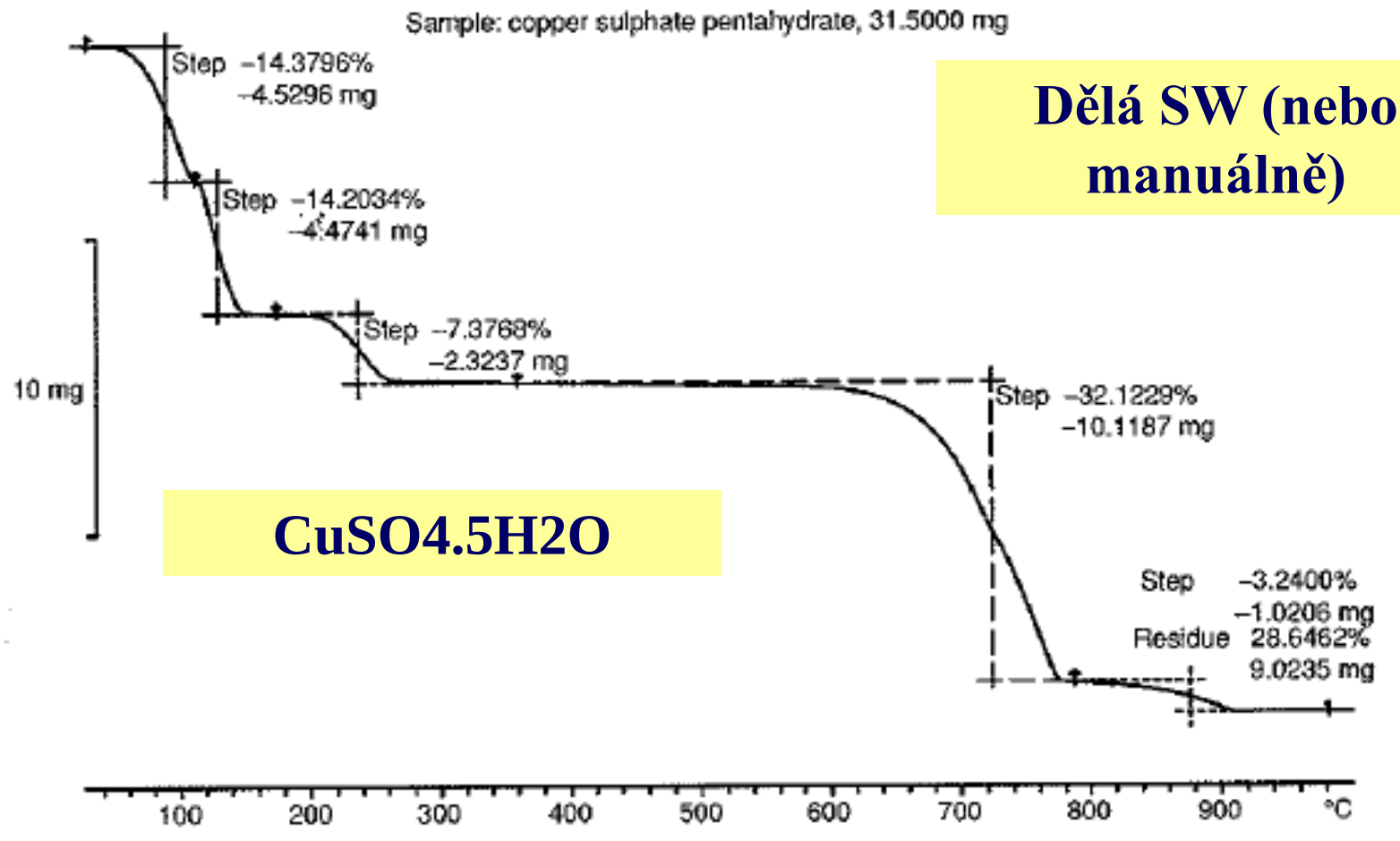

Dělá SW (nebo manuálně)

CuSO4.5H2O

Figure 3.14 Separation in a TGA curve of copper sulphate pentahydrate at 10 K/min. The individual steps correspond to the consecutive elimination of the following molecules: 2 H_2O, 2 H_2O, 1 H_2O, SO_3, 0.5 O_2. The residue is Cu_2O.

Příprava karamelu

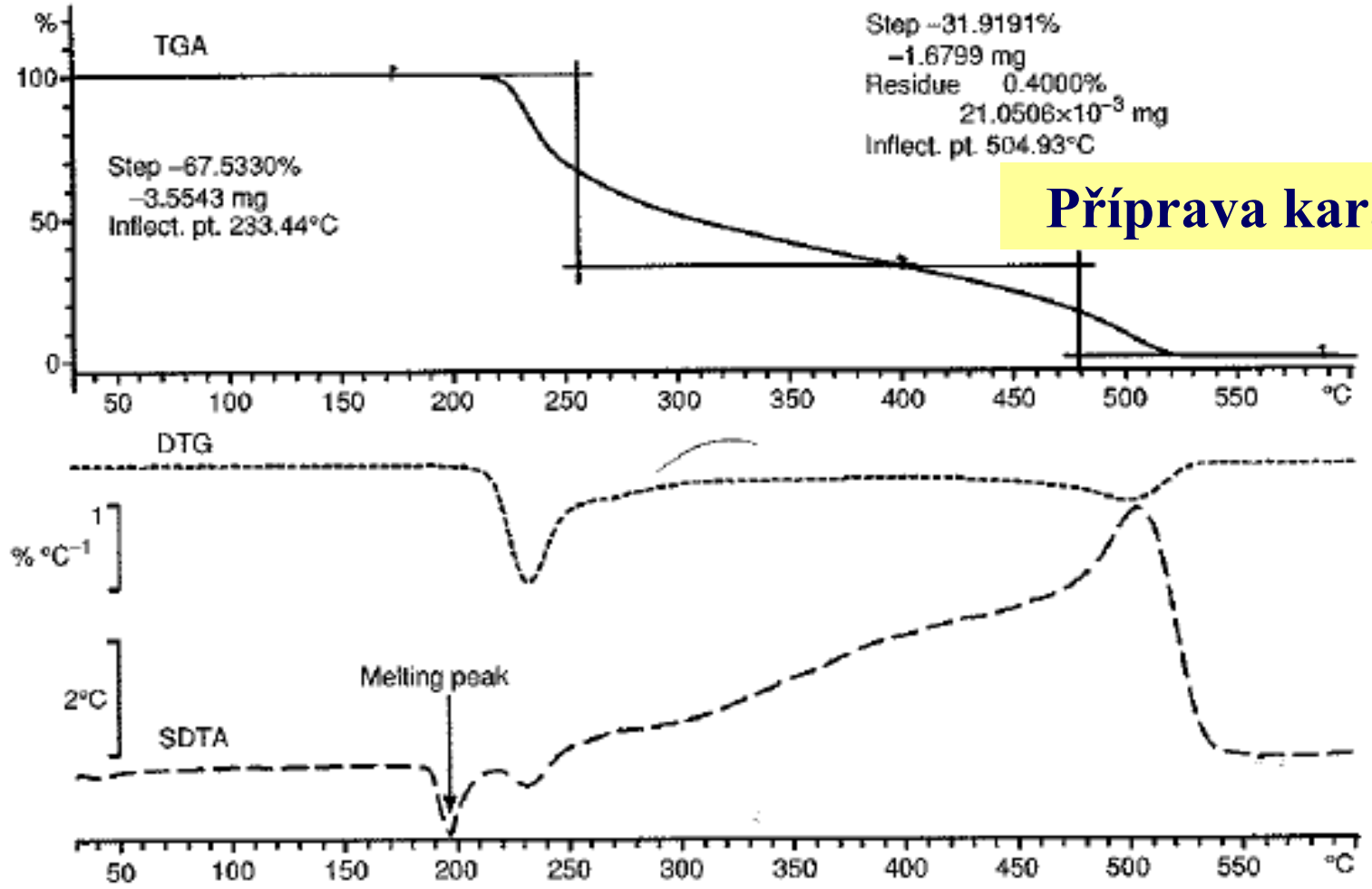

Figure 3.15 The decomposition of sucrose at 10 K/min in air occurs in two consecutive steps, the second directly following the first. In the evaluation, a value of 405°C was used for the end of the first step and the beginning of the second step. The simultaneously measured SDTA curve shows the endothermic melting peak followed by the endothermic caramelisation, at which stage the exothermic decomposition/combustion occurs. An almost white residue of 0.4% remains at the end of the measurement. This corresponds to the ash content.

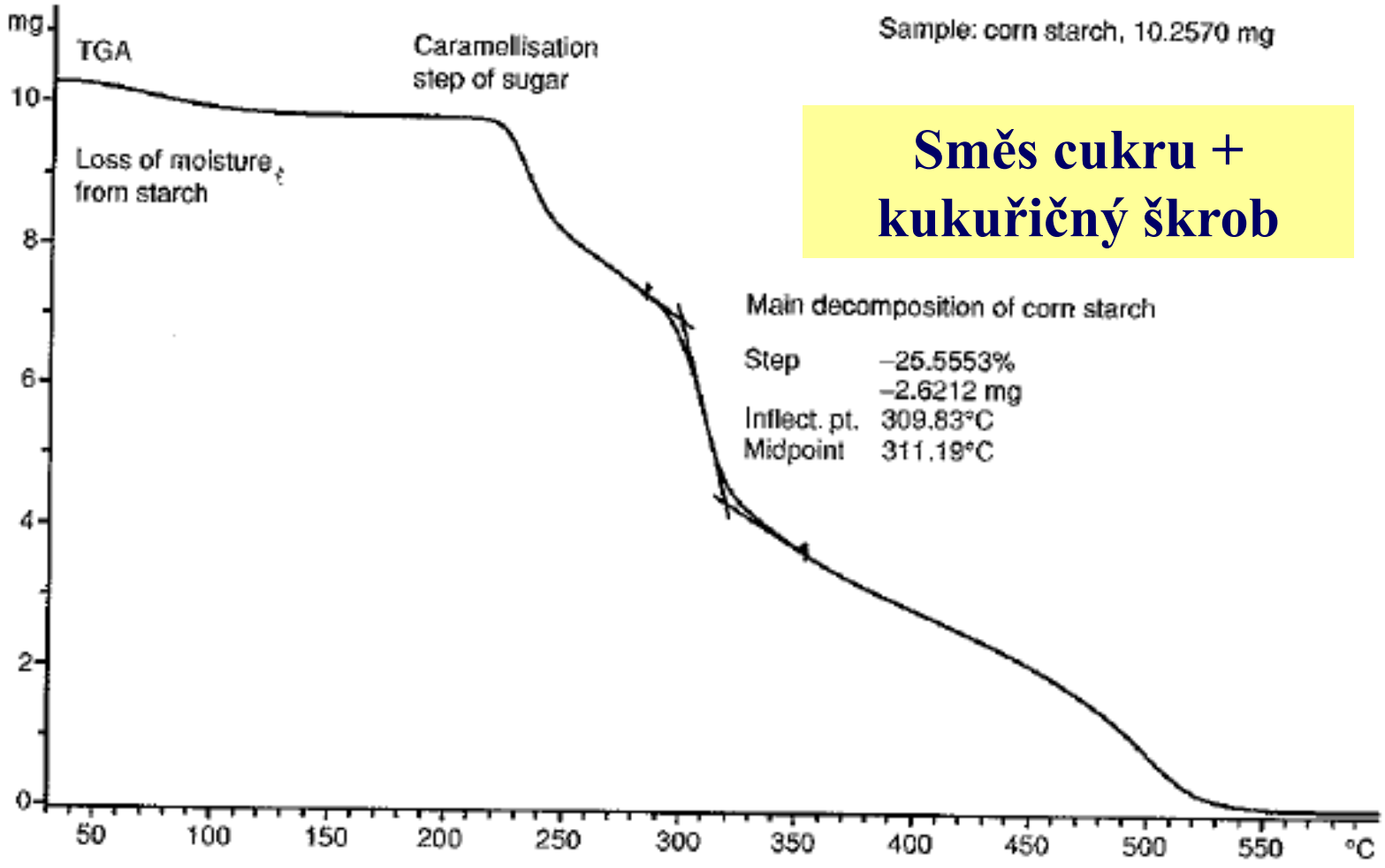

Figure 3.16 TGA curve of a 1:1 mixture of maize-corn starch and crystalline sugar: heating rate 10 K/min, purge gas air at 50 mL/min. The main decomposition step of corn starch occurs at roughly 310°C (midpoint). In a mixture with crystalline sugar, the 'starch' step occurs in a region in which the mass of the sugar continuously decreases. The step obtained using a 'horizontal' evaluation would be too large. This error can be avoided using a 'tangential' baseline evaluation. The measured step of 25.5% refers to the initial total mass of the mixture at the beginning of the measurement (see Section 3.6.3).

Metodika vyhodnocení TGA

Změna hmotnosti v %:

$$G\% = 100.\Delta m/m_0$$

Stupeň přeměny reakce (solid state reakce např oxidace, rozklad,…)

$$\alpha = \frac{m_0 - m}{m_0 - m_f}$$

m_0, m_f and m

Počáteční, konečná a aktuální hmotnost

Rychlostní rovnice přeměny

$$\frac{d\alpha}{dt} = kf(\alpha)$$

Integrovaná rychlostní rovnice přeměny

$$g(\alpha) = \int_0^{\alpha} \frac{d\alpha}{f(\alpha)} = kt$$

Obecně pro isotermní i neisotermní ohřevy platí:

$$\frac{d\alpha}{dt} = A \exp\left(-\frac{E_a}{RT}\right) f(\alpha) a(\alpha, T, P, \ldots.)$$

***a*…akomodační funkce (často=1)**

TGA ovlivněné nukleací a růstem nové fáze

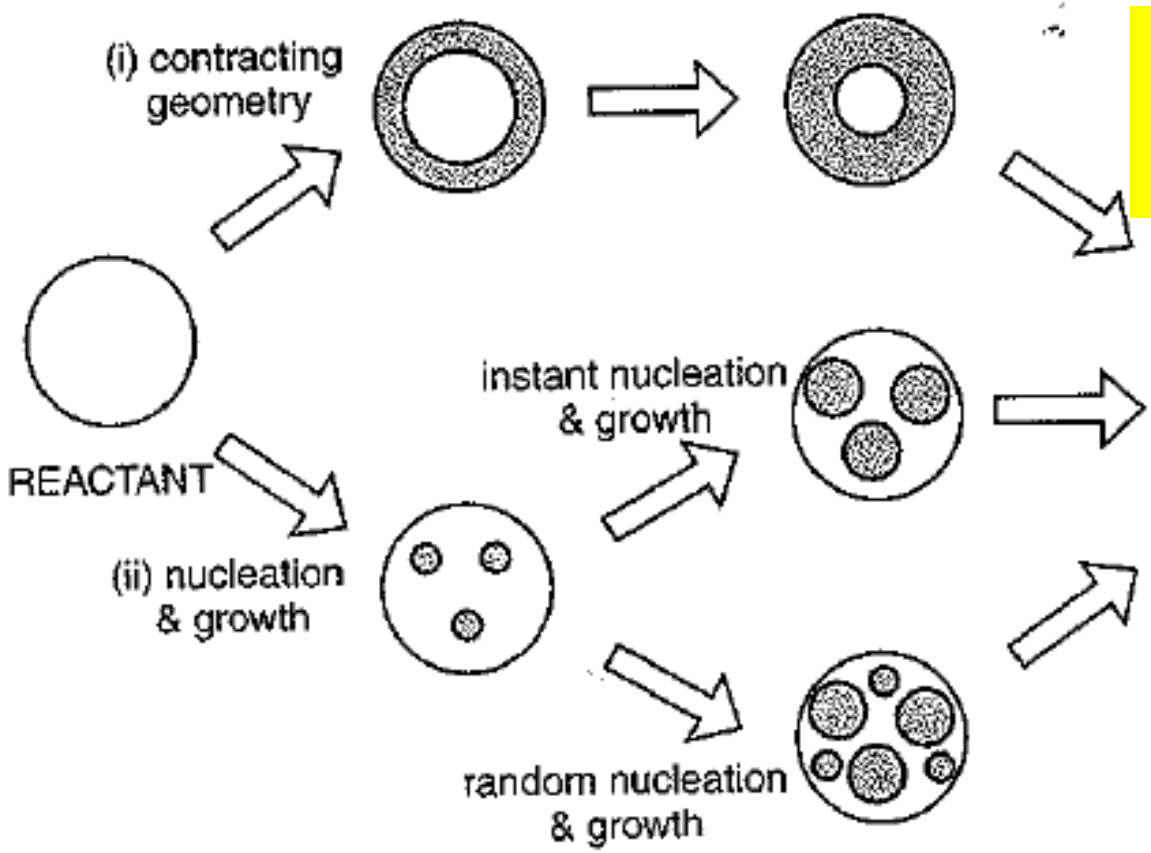

Kontrolováno difúzí (Dn) nebo růstem rozhraní (Rn)

Kontrolováno nukleací, difúzí a růstem (An)

Figure 1 Schematic representation of the contracting geometry and nucleation–growth models

Cesta A: např. oxidace,
cesta B např. vznik hydridů

TGA and typical mass changes

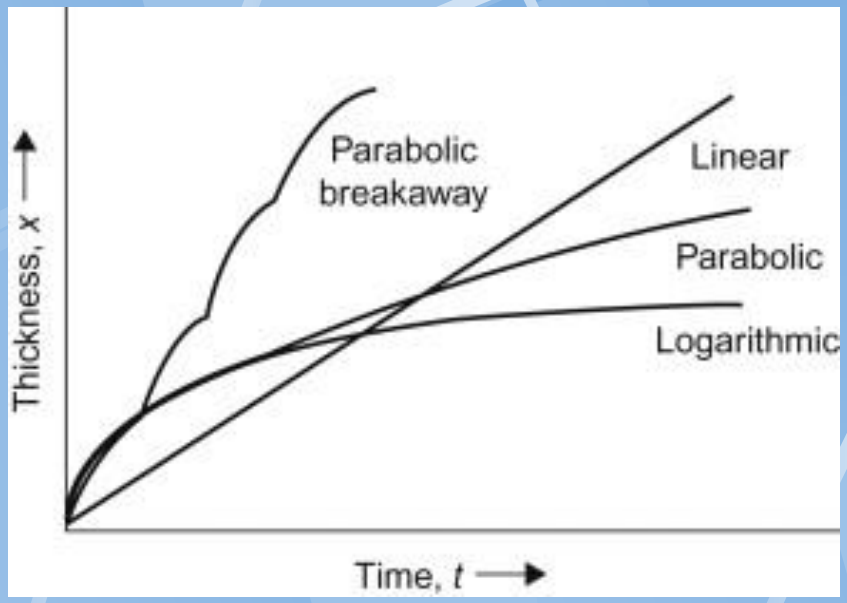

[Parabolic Rate Law - an overview | ScienceDirect Topics]

Pro příliš časově náročné experimenty se TGA nepoužívá

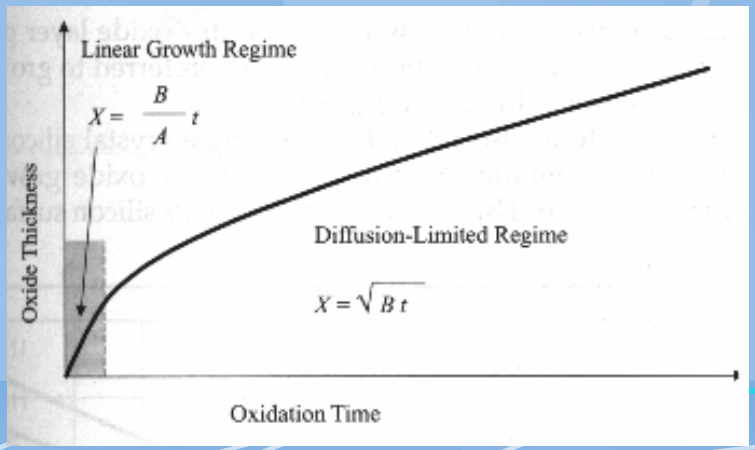

[Linear and Parabolic Rate Constants (jhaj.net)]

Studium ocelí

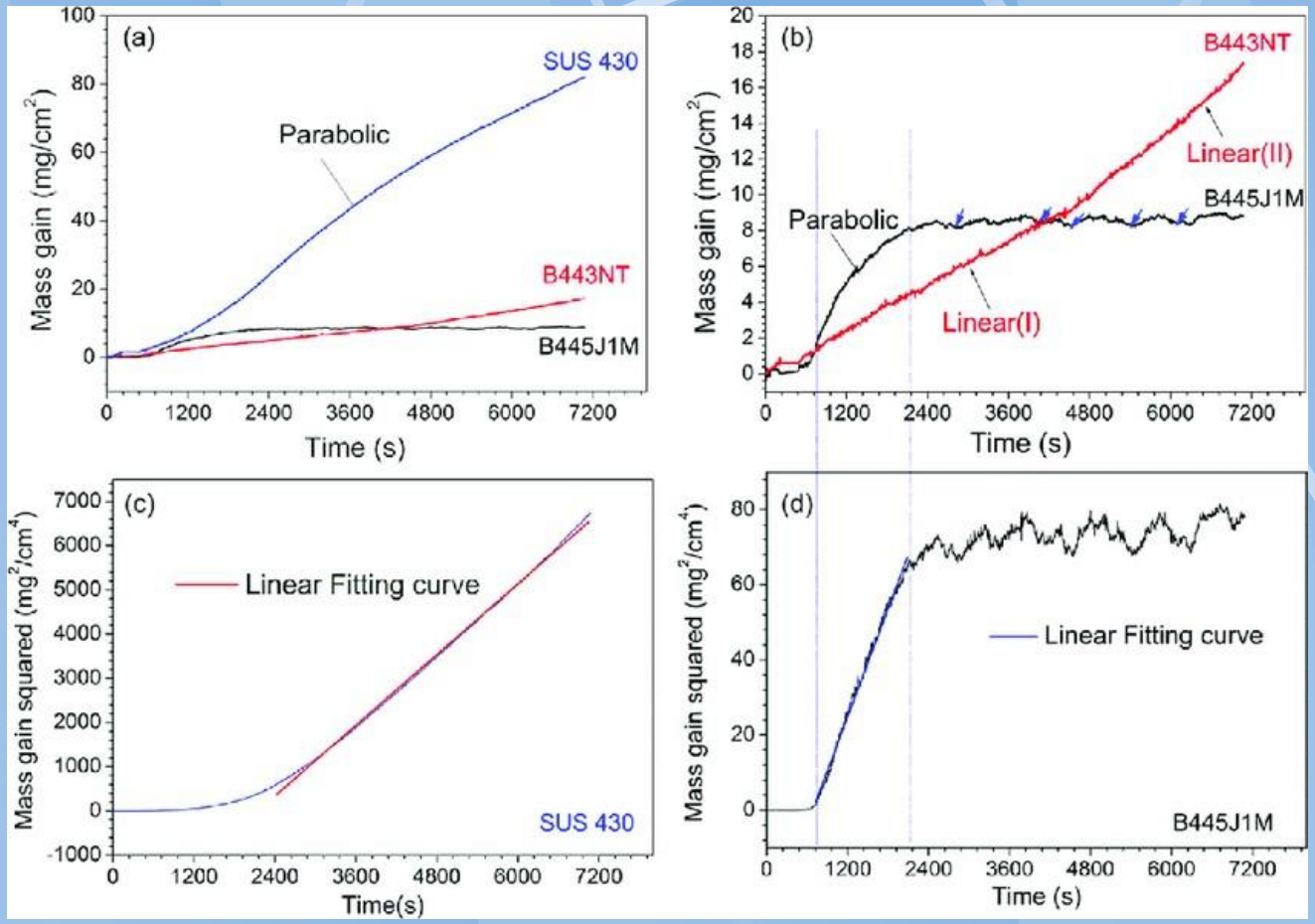

TGA curves of three ferritic stainless steels oxidised at 1200 °C for 7200 s in air. (a) Δm/s-t plots, (b) the detailed Δm/s-t plots of the B443NT and B445J1M steels, (c) parabolic plot (Δm/s) 2-t of the SUS430 steel and (d) parabolic plot (Δm/s) 2-t of the B445J1M steel. [Color figure can be viewed at wileyonlinelibrary.com]

TGA curves of three ferritic stainless steels oxidised at 1200 °C for... | Download Scientific Diagram (researchgate.net)

Isotermní ohřev a vyhodnocení kinetiky

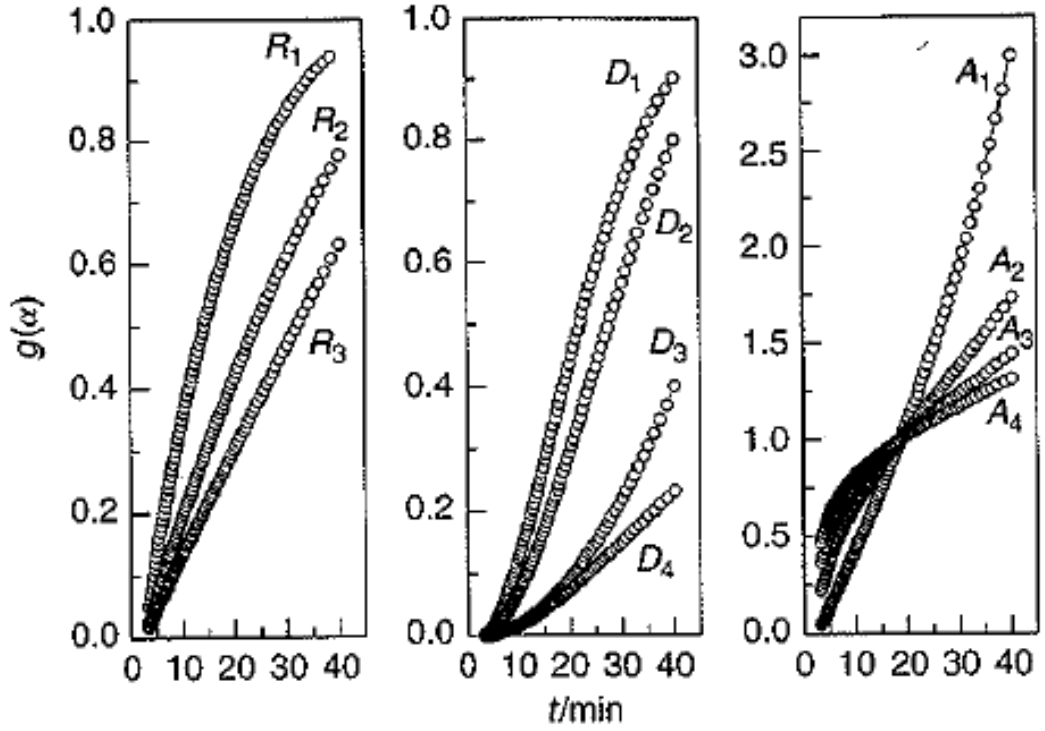

Figure 1 Typical plots of $g(\alpha)$ against t for the isothermal dehydration of zinc acetate dihydrate

Dehydratace Zn Ac.2H2O

Z křivek určíme *k* za dané teploty pro různé teploty platí:

$$\ln k = \ln A - \frac{E_a}{RT}$$

Určení typu kinetiky pro isotermní ohřev

Table 1 Typical kinetic model functions derived for the solid-state reactions

Model	Symbol	$f(\alpha)$	$g(\alpha) = \int_0^\alpha \frac{d\alpha}{f(\alpha)}$
Phase boundary controlled reaction	R_n ($n = 1$, 2 or 3)	$n(1-\alpha)^{1-1/n}$	$1-(1-\alpha)^{1/n}$
1D diffusion	D_1	$\frac{1}{2\alpha}$	α^2
2D diffusion	D_2	$-\frac{1}{\ln(1-\alpha)}$	$\alpha + (1-\alpha)\ln(1-\alpha)$
3D diffusion (Jander)	D_3	$\frac{3(1-\alpha)^{2/3}}{2[1-(1-\alpha)^{1/3}]}$	$[1-(1-\alpha)^{1/3}]^2$
3D diffusion (Ginstring–Brounshtein)	D_4	$\frac{3}{2[(1-\alpha)^{-1/3}-1]}$	$1-\frac{2\alpha}{3}-(1-\alpha)^{2/3}$
Nucleation and growth (Avrami–Erofeev)	A_m ($m = 0.5$, 1, 1.5, 2, 2.5, 3 or 4)	$m(1-\alpha)[-\ln(1-\alpha)]^{1-1/m}$	$[-\ln(1-\alpha)]^{1/m}$

Zjistíme, který model vyhovuje z linearizovaných tvarů *f* a *g* a určíme typ kinetiky.

Určení typu kinetiky pro neisotermní ohřev (např. lineární)

Table 1 Typical methods of kinetic analysis for nonisothermal data

Methods	Form	Reference	Approximation	Kinetic equation
Single run	Differential	Achar *et al.*[4]	non	$\ln\left[\frac{d\alpha}{dt}\frac{1}{f(\alpha)}\right] = \ln A - \frac{E_a}{RT}$
	Integral	Coats and Redfern[5]	$p(x)$	$\ln\frac{g(\alpha)}{T^2} = \ln\left[\frac{AE_a}{\beta R}\left(1-\frac{2RT}{E_a}\right)\right] - \frac{E_a}{RT}$
Isoconversional	Differential	Friedman[6]	non	$\ln\frac{d\alpha}{dt} = \ln[Af(\alpha)] - \frac{E_a}{RT}$
	Integral	Ozawa[7]	$p(x)$	$\log\beta = \log\frac{AE_a}{g(\alpha).R} - 2.315 - 0.4567\frac{E_a}{RT}$
Peak	2nd differential	Kissinger[8]	$f(\alpha) = -\ln(1-\alpha)$	$\ln\frac{\beta}{T_p^2} = \ln\left[\frac{df(\alpha_p)}{d\alpha}\frac{AR}{E_a}\right] - \frac{E_a}{RT_p}$

Detaily viz lit. Sorai

Časté aplikace TGA

Zajímá nás	Z TGA křivky vyhodnocujeme
Effect, property of interest	Evaluation used
Composition	Step evaluation, residue
Thermal stability, decomposition	Step evaluation
Stoichiometry of reactions	Content
Kinetics of reactions	Conversion, kinetics
Adsorption/desorption processes	Step evaluation
Vaporisation behaviour	Step evaluation, DTA, integration
Influence of reactive gases	Step evaluation
Moisture	Step evaluation
Oxidation stability	Onset

Example – oxidation of pure Cr

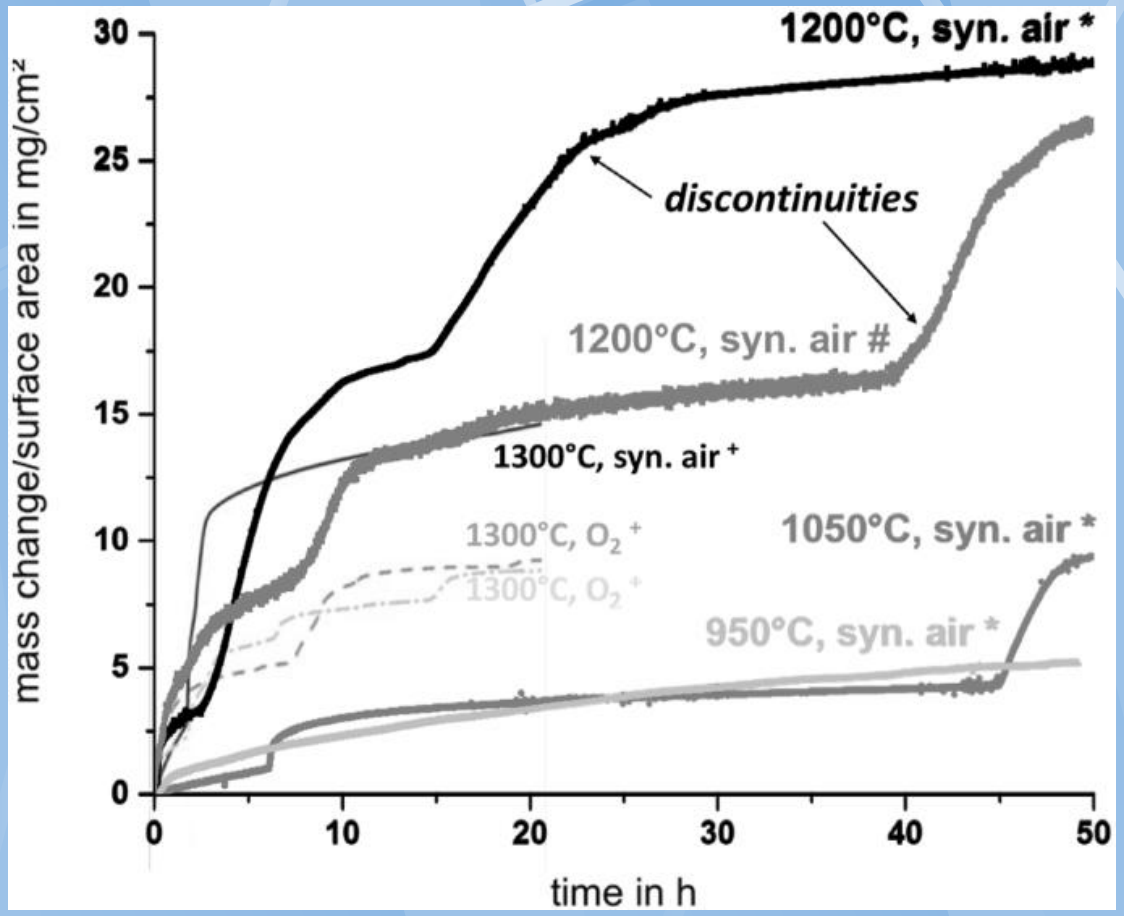

Mass change measurements of pure Cr during oxidation in synthetic air or pure oxygen. Taken from + [2], * [3], and # [4]

Vznik více vrstev různých oxidů

Discontinuities in Oxidation Kinetics: A New Model and its Application to Cr–Si-Base Alloys | High Temperature Corrosion of Materials (springer.com)

Stanovení vlhkosti vzorku

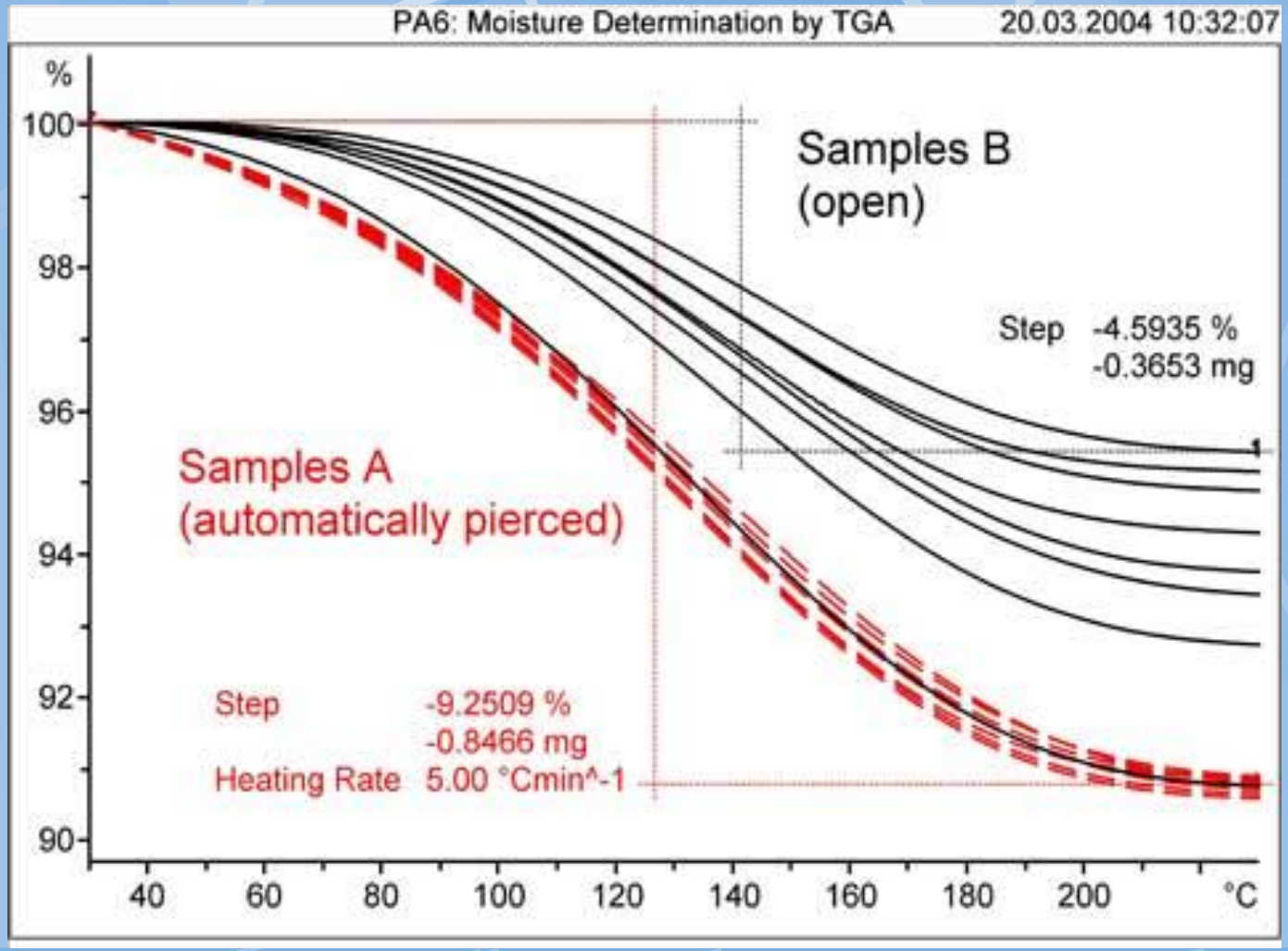

Vlhkost 4,59%

Vlhký cca 9,25%

Diskuze

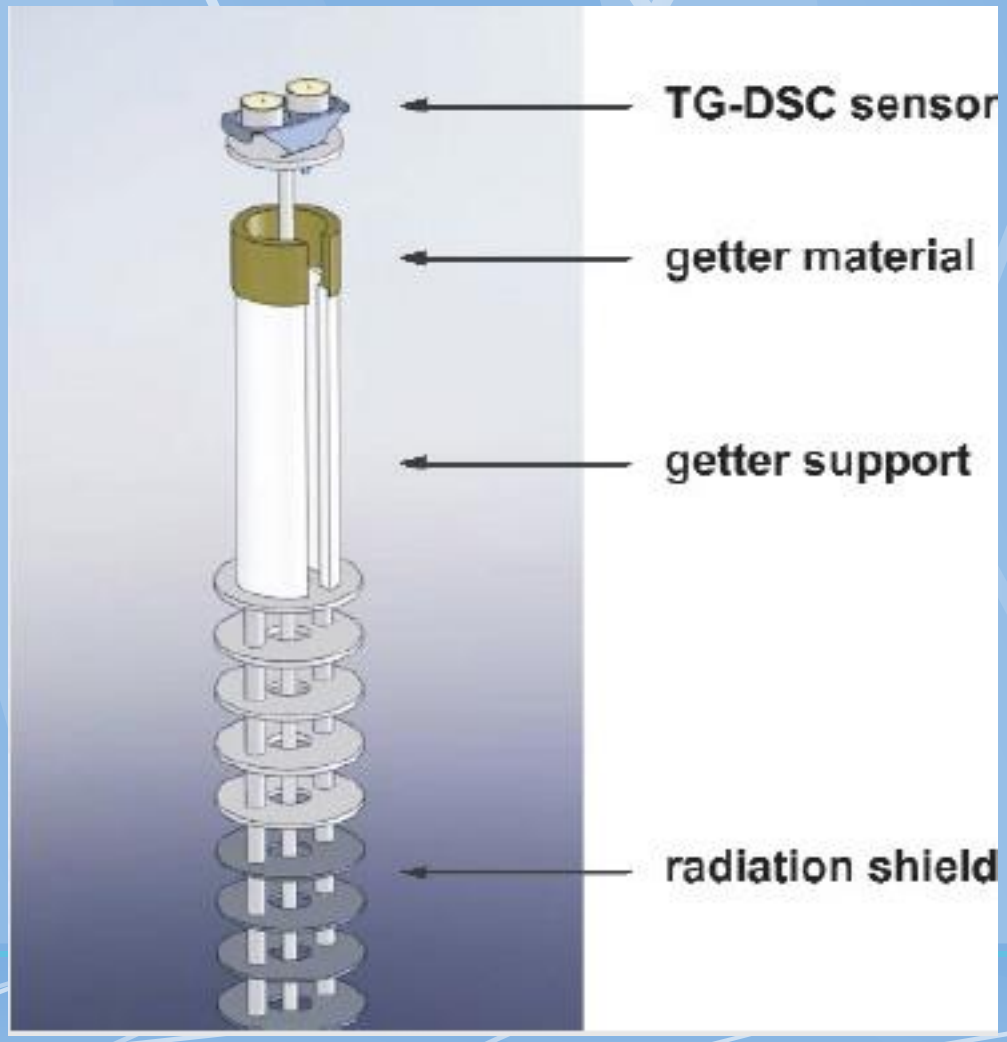
TG-DSC sensor
getter material
getter support
radiation shield